A Possible Effect of an Increase in the Warm-Pool SST on the Magnitude of El Niño Warming

DE-ZHENG SUN

NOAA–CIRES/Climate Diagnostics Center, Boulder, Colorado

(Manuscript received 16 November 2001, in final form 22 July 2002)

ABSTRACT

El Niño warming corresponds to an eastward extension of the western Pacific warm pool; one thus naturally wonders whether an increase in the warm pool SST will result in stronger El Niños. This question, though elementary, has not drawn much attention. The observation that the two strongest El Niños in the instrumental record occurred during the last two decades, when the warm pool SST was anomalously high, however, has added some urgency to answering this question. Here observational and numerical results that support a positive answer to this question are shown.

The observational results come from an analysis of the heat balance of the tropical Pacific over the period 1980–99. The analysis confirms that El Niño acts as a major mechanism by which the tropical Pacific transports heat poleward—the poleward heat transport is achieved episodically, and those episodes correspond well with the occurrence of El Niños. Moreover, the analysis shows that El Niño is a regulator of the heat content in the western Pacific: the higher the heat content, the stronger the subsequent El Niño warming, which transports more heat poleward, and results in a larger drop in the heat content in the western Pacific. These empirical results suggest that a higher warm-pool SST may result in stronger El Niño events. Specifically, raising the tropical maximum SST through an increase in the radiative heating across the equatorial Pacific initially increases the zonal SST contrast. A stronger zonal SST contrast then strengthens the surface winds and helps to store more heat in the subsurface ocean. Because of the stronger winds and the resulting steeper tilt of the equatorial thermocline, the coupled system is potentially unstable and is poised to release its energy through a stronger El Niño warming. A stronger El Niño then pushes the accumulated heat poleward and prevents heat buildup in the western Pacific, and thereby stabilizes the coupled system.

Numerical experiments with a coupled model in which the ocean component is a primitive equation model (the NCAR Pacific basin model), and therefore explicitly calculates the heat budget of the entire equatorial upper ocean, support this suggestion. The numerical experiments further suggest that in the presence of El Niños, the time-mean zonal SST contrast may not be sensitive to increases in the surface heating because the resulting stronger El Niños cool the western Pacific and warm the eastern Pacific.

1. Introduction

The tropical maximum SST—the SST in the western Pacific warm pool—has been anomalously higher in the last two decades. The two strongest El Niños in the century-long instrumental record—the 1982/83 and 1997/98 El Niño also occurred within this period (Fig. 1). Are the exceptional strength of the 1982/83 and 1997/98 El Niños possibly due to the anomalously higher warm-pool SST? Given the fact that El Niño warming corresponds to an eastward extension of the warm pool, one naturally wonders whether an increase in the warm-pool SST will result in stronger El Niños.

The need to better understand the effect of an increase in the warm-pool SST on the amplitude of ENSO is further highlighted by the concern with how ENSO will respond to global warming. By comparing the time series of the tropical maximum SST in Fig. 1a with the time series of the global mean air temperature (Houghton et al. 2001, Fig. 1a of the Summary for Policymakers), one notes that the warm-pool SST has been warming up over the last century in a very similar fashion to the global mean surface air temperature. This similarity includes the rapid warming in the early part of the twentieth century and the rapid warming in the last two decades. The warming trend in the global mean surface air temperature has been in part attributed by Houghton et al. (2001) to the effect of anthropogenic forcing. Given the striking similarity between the two time series, it is hard to imagine that the trend in the tropical maximum SST could be entirely free from the influence of global warming. Thus understanding the effect of an increase in the warm-pool SST on the magnitude of El Niño may be an important step toward fully addressing the question of

Corresponding author address: Dr. De-Zheng Sun, NOAA/ERL/CDC, (R/E/CDC1), Climate Diagnostics Center, 325 Broadway, Boulder, CO 80303.
E-mail: ds@cdc.noaa.gov

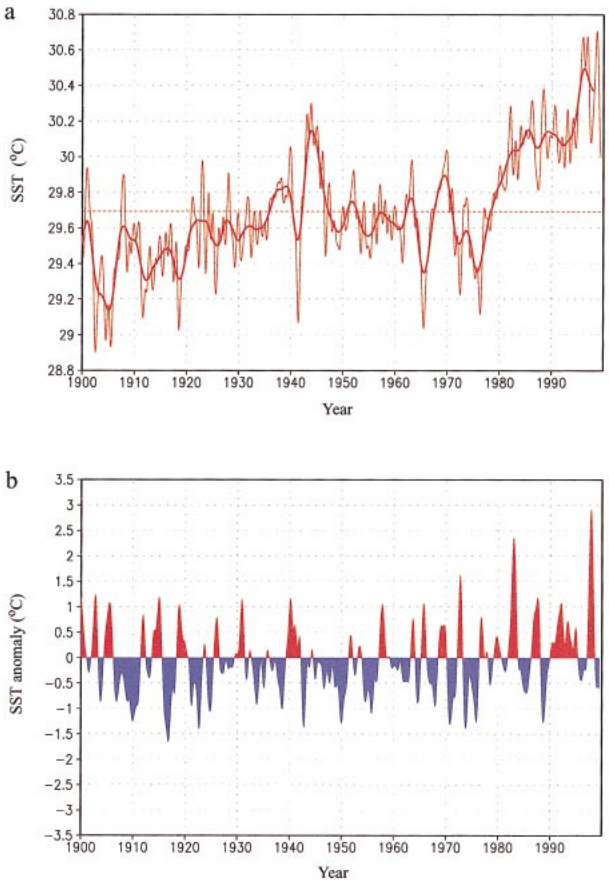

FIG. 1. (a) Variations of the tropical maximum SST (SST_{max}) over the last century. SST_{max} is obtained here by finding the maximum value of SST within the western Pacific warm pool region (5°S–5°N, 120°–160°E). Shown are data smoothed by a cosine bell window with a width of 13 months (thin line) and a width of 49 months (thick line). (b) Interannual anomalies of Niño-3 (5°N–5°S, 90°–150°W) SST for the same period. SST data are from the Hadley Centre for Climate Prediction and Research (Rayner et al. 1996).

whether El Niño would become more energetic in response to global warming.

There are additional reasons to pay particular attention to the anomalously high warm-pool SST in the last two decades. Note that the interannual variability in the center of the warm pool is small. Consequently, the distinct warming over the last two decades in the tropical maximum SST is unlikely a consequence of stronger El Niño events during this period. The same cannot be said for the warming trend in the eastern equatorial Pacific where El Niño signals dominate the variability in the SST. The seemingly anomalously warm SST over the last two decades in the equatorial eastern Pacific could be largely due to the stronger El Niño events during this period. Cane et al. (1997) showed that with the effect of the El Niños removed, the eastern equatorial Pacific SST actually has a negative trend over the last century. After the 2–7-yr signal is removed from the SST of the last 50 yr through the use of a bandpass filter, no significant trend is detected in the eastern equatorial Pacific SST. Clearly, further study is needed to settle whether there is a significant warming trend in the eastern equatorial Pacific that is not due to the recent stronger El Niño events.

A positive relationship between the tropical maximum SST and the amplitude of ENSO was hypothesized by Sun (1997). In an attempt to establish a theoretical basis for the empirically derived notion that El Niño may be a mechanism by which the equatorial ocean transports heat poleward (Sun and Trenberth 1998), Sun (1997) constructed a simple mathematical model of the tropical Pacific that includes the delayed oscillator physics (Zebiak and Cane 1987; Battisti 1988; Suarez and Schopf 1988; Jin 1997a,b), but calculates the total SST. Following earlier theoretical studies, the surface heat flux is parameterized to be proportional to the differences between the tropical maximum SST and the actual SST (Neelin et al. 1998). Thus an increase in the tropical maximum SST in the model is equivalent to an increase in the net surface heating across the equatorial Pacific. The deep ocean temperature is fixed in the model. Sun (1997) found in this model that El Niño-like oscillations only occur when the tropical maximum SST exceeds a critical value—a value that is very close to the observed one—and that the magnitude of El Niño warming increases with further increases in the tropical maximum SST. The model, however, is a highly simplified one. Nonetheless, the results appear to be consistent with an earlier result from the study with the use of a more sophisticated model—the intermediate model of Zebiak and Cane (1991). Using their pioneering model for ENSO, they found that a warmer SST in the background state supports more energetic ENSO. In a more recent study using the same model, however, Clement et al. (1996) found that ENSO in the model actually becomes weaker in response to an increase in the surface heating. [The increase in the surface heating was achieved through an uniform increase in the restoring SST across the model domain (30°S–30°N)]. The apparent discrepancy between these two studies may not be serious because the resulting changes in the mean state in experiments with enhanced heating of Clement et al. (1996) may be different from those imposed in the study of Zebiak and Cane (1991). Note that intermediate models for ENSO do not have a heat budget for the subsurface ocean, and consequently the subsurface temperature (T_{sub}) has to be parameterized. Thus the response of ENSO as well as the mean state in an intermediate model to an increase in the surface heating could be very sensitive to the details of how T_{sub} is parameterized. In fact, Sun (2000a) suggested that the differences between the results from Sun (1997) and the study by Clement et al. (1996) could be partially due to the differences in the way T_{sub} was parameterized (or equivalently how the subsurface ocean feels the additional heating imposed on the surface of the ocean). The uncertainty associated with the empirical parameterization of T_{sub}

may not be removed unless the ocean model used has an explicit heat budget for the subsurface ocean.

The results from fully coupled GCMs are more mixed. Early studies by Knutson et al. (1997), Tett (1995), and Meehl et al. (1993) suggest that global warming may result in little changes in the amplitude of ENSO. A recent study by Timmermann et al. (1999), however, shows that at least in their model, the amplitude of ENSO increases significantly in response to global warming. Since the model of Timmermann et al. (1999) has a finer resolution in the Tropics than earlier GCMs, the later results may be more reliable. In light of the sensitivity results from the model of Zebiak and Cane (1987), Timmermann singled out the changes in the vertical stratification in the upper thermocline as a potential candidate to be responsible for the enhanced ENSO variability. As they further discussed, however, there were many other significant changes in the model mean state that may or may not work in the same direction as the vertical stratification. Consequently, a casual relationship is hard to ascertain from their study. What appears to be needed is a study using a simpler model with a simpler forcing. Using a model that is capable of calculating the heat budget of the entire upper ocean, and yet allows the tropical maximum SST to be changed easily then emerges as a reasonable start in that direction. While we acknowledge that global warming is potentially a more complex forcing than a simple increase in the tropical maximum SST or the surface heating in the equatorial region, we also would like to point out that the increases in the topical SST over the last 50 yr are confined to the equatorial region—the subtropical and extra-tropical SSTs are actually somewhat colder (Zhang et al. 1997). (To the extent the eastern equatorial Pacific SST is connected to the subtropical/extratropical SST on the decadal and longer timescales, the cooling in the subtropical/extratropical SST further suggests that the anomalous warming in the eastern equatorial Pacific is the effect of the strong El Niño events during this period.) Thus studying the impact of a warmer warm-pool SST on the amplitude of ENSO may be more relevant for understanding how ENSO responds to global warming than it may first appear to be.

To date, fully coupled GCMs have not been used to single out the effect of an increase in the tropical maximum SST and consequently the effect of an enhanced surface heating over the equatorial Pacific on the magnitude of El Niño warming. The technical difficulty for such a study has probably been the obstacle. Nonetheless, in comparing the National Center for Atmospheric Research Climate System Model (NCAR CSM) simulations of the present climate with observations, one notes a positive relationship between the warm-pool SST and the amplitude of ENSO: the CSM has a colder warm-pool SST (Kiehl 1998), it also has a much weaker ENSO (Boville and Gent 1998; Meehl and Arblaster 1998). Of course, both the cold bias in the warm-pool SST and the underestimate of ENSO could be a result of inaccuracies in the model physics, such as the cumulus parameterization scheme, rather than one being the cause of the other. This again speaks of the need for a study that is specifically designed to address the influence of the warm-pool SST on the magnitude of El Niño warming.

The present study attempts to fulfill such a need—to better ascertain and understand the effect of an increase in the warm-pool SST on the amplitude of ENSO. We attempt to achieve this objective through combining observational data with focused numerical experiments. We note at the very beginning that the tropical maximum SST is fundamentally linked to the surface heat flux into the equatorial ocean. First, the equatorial surface heat flux F_s appears to be well represented by the traditional formula $F_s \approx \mathrm{SST}_p - \mathrm{SST}$ where SST_p is the SST the surface ocean would have attained in the absence of any ocean dynamics. (SST_p has been termed the radiative–convective equilibrium SST by previous studies, emphasizing its close relationship with the radiative heating.) This formula has been widely used in earlier theoretical studies (Neelin et al. 1998) and is supported by the most recent calculations of the equatorial surface heat flux (Trenberth 1997). Since the net heat flux in the center of the warm pool is nearly zero (Ramanathan et al. 1995; Gent 1991), the maximum SST is close to SST_p. Model results generally show that raising SST_{max} through increasing SST_p increases the zonally averaged heat flux into the equatorial ocean (Sun and Liu 1996; Clement et al. 1996; Seager and Murtugudde 1997). With the consideration of the close relationship between the tropical maximum SST and the equatorial surface heating, we will first proceed with empirical results from an analysis of the heat balance of the tropical Pacific over the last 20 yr. These empirical results further substantiate the notion that El Niño represents a major mechanism by which the equatorial upper ocean transports heat poleward. This finding suggests a specific link between the tropical maximum SST (T_{max}) and the magnitude of El Niño warming as they both are involved in a fundamental way in the heat balance of the tropical Pacific. The empirical results also show that El Niño acts as a regulator of the heat content in the western Pacific, adding another important detail to how the warm-pool SST may influence the magnitude of El Niño warming. The empirical results also highlight the role of the equatorial cold tongue or the role of La Niña in helping the ocean to store heat absorbed at surface to the subsurface ocean, the subsurface ocean in the western Pacific in particular. Combining these results, we envision the following scenario concerning the response of ENSO to an increase in the tropical maximum SST. An increase in the tropical maximum SST initially results in an increase in the zonal SST contrast through the mechanism of Sun and Liu (1996) and Clement et al. (1996). A stronger zonal SST contrast then strengthens the surface winds. Because of the stronger winds and the resulting steeper tilt of the equatorial thermo-

cline, the coupled system not only has more heat stored in the western Pacific, but also is more potentially unstable, and is thus poised to release its energy through a stronger El Niño warming. A stronger El Niño then pushes the accumulated heat poleward and prevents heat buildup in the western Pacific and thereby stabilizes the coupled system. We test this hypothesis using a coupled model in which the ocean component is a primitive equation model and therefore explicitly calculates the heat budget of the entire upper ocean. We finally discuss the implications of the present study and also point out potential caveats.

2. Observational results

a. The role of El Niño in heat removal from the equatorial Pacific

El Niño warming occurs in the part of the tropical Pacific where there is strong surface heating. Using bulk formulas and marine weather observations, Weare et al. (1981) calculated the annual mean surface heat flux over the tropical Pacific. The calculation revealed that the tropical Pacific is strongly heated in the equatorial region (and cooled in the higher latitudes). More recent calculations using a residual method (Trenberth 1997; Sun and Trenberth 1998) and direct output from National Centers for Environmental Prediction–NCAR (NCEP–NCAR) reanalysis (Kalnay et al. 1996) confirm this feature (Figs. 2a and 2b). Figures 2a,b imply that the ocean has to remove heat away from the equatorial ocean to the higher-latitude ocean. Is El Niño a basic process in this poleward heat removal?

The heat balance in the equatorial Pacific has been traditionally described in terms of poleward surface Ekman flow and the returning subsurface geostrophic flow. Figure 2.1 in Philander (1990) typifies this description. While this picture is meant to represent the time-mean circulation, it nevertheless carries an implication that the poleward heat removal is achieved by a steady circulation. In fact, a very recent study by Klinger and Marotzke (2000) apparently assumed that this was indeed the situation. As we will see more clearly, the heat removal from the equatorial Pacific is not constant in time. The poleward heat transport is achieved more in an episodic fashion, and those episodes apparently have a good correspondence with the occurrences of El Niños. We will suggest that El Niño is a mechanism by which the equatorial ocean transports heat poleward in the same sense as cumulus convection transports energy upward away from the surface boundary layer. This analogy then allows us to see from a new perspective what controls the stability of the coupled equatorial tropical ocean–atmosphere, and why the tropical maximum SST is an important parameter in determining the magnitude of El Niño warming.

Wyrtki (1985) was probably the first who suggested a possible link between El Niño and the heat balance

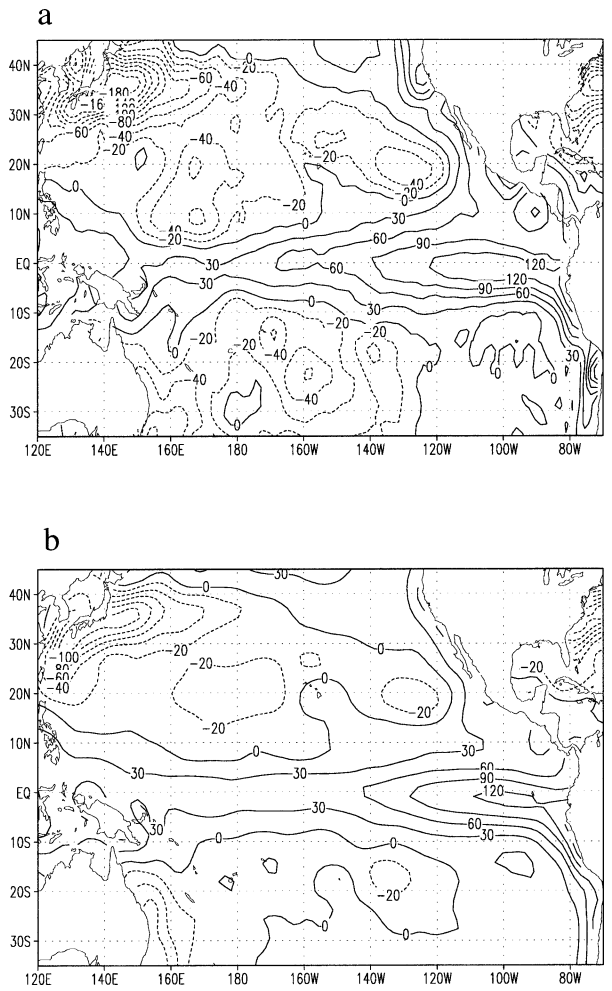

FIG. 2. (a) Distribution of annual mean surface heating over the Pacific Ocean inferred from the the energy balance of the atmosphere over the ERBE period (Sun and Trenberth 1998). (b) Distribution of surface heating from the NCEP–NCAR reanalysis for the same period (Kalnay et al. 1996). Data in (a) and (b) are smoothed by a nine-point filter and have units of W m^{-2}.

of the tropical Pacific. He noted that at the end of the 1982/83 El Niño, warm water in the equatorial Pacific was depleted and was lost to higher latitudes. This result suggested a heat discharge toward higher latitudes during the 1982/83 El Niño. A more quantitative picture for the discharge of heat during El Niño was given by Sun and Trenberth (1998) who compared the differences in the poleward heat transport in the ocean between 1987 (an El Niño year) and 1985 (a normal year) with the concurrent changes in the shortwave cloud forcing and in the transport of moist static energy in the atmosphere. They found that the increases in the poleward heat transport in the ocean are four times as large as the increases in the cloud reflection of solar radiation. The large heat loss to the higher latitudes then raises the question of where the heat removed during the El Niño warming comes from in the first place. Extending the analysis of

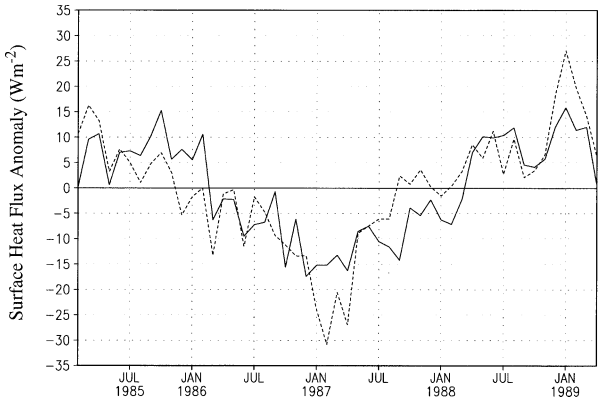

FIG. 3. Interannual anomalies of NCEP surface heat flux over the equatorial Pacific (5°S–5°N) over the ERBE period. The dashed line is the surface heat flux used in Sun (2000b) and Sun and Trenberth (1998).

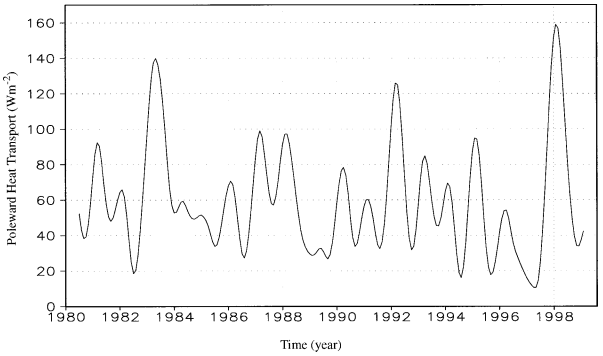

FIG. 4. Poleward ocean heat transport out of the equatorial region (5°S–5°N). A Hanning window (a cosine bell window) with a width of 13 months was used to smooth the data.

the heat balance of the tropical Pacific to the entire Earth Radiation Budget Experiment (ERBE) period, Sun (2000b) showed that the heat removed comes from the accumulated heat in the upper ocean, which in turn comes from the surface heating. During the cold phase, the surface heat flux into the ocean is strong while the poleward transport of heat is weak, resulting in accumulation of heat in the upper ocean. The accumulated heat then resurfaces in the eastern equatorial Pacific through the undercurrent, and upwelling and El Niño warming develops. The ensuing rapid zonal redistribution of heat in the equatorial Pacific results in a thermal structure that enhances the poleward heat transport across the basin. The large increase in the poleward heat transport incurred by El Niño eventually plunges the system into a cold state and the ENSO cycle starts again. The results thus reinforce the impression that the heat removal from the equatorial Pacific may be divided into two stages—a preparation stage and an actual removal stage—and that El Niño may be a basic mechanism by which the ocean transports heat poleward. The analysis period of Sun (2000b), however, only covers one ENSO cycle. Consequently, whether transporting heat poleward episodically is a defining feature in the maintenance of the long-term heat balance of the tropical Pacific, and whether El Niño events have a general good correspondence with the transporting episodes, are not yet concretely known.

In this paper, we extend the calculation of the heat budget of the tropical Pacific to the last 20 yr over which ocean temperature data from the NCEP assimilation system are available (January 1980–August 1999; Ji et al. 1995). This period covers six El Niños among which the 1982/83 and the 1997/98 El Niño were exceptionally strong. In this section, we first attempt to address the following two questions: 1) Do all El Niños in the extended period of analysis correspond to an elevated level of poleward heat transport? 2) Are stronger El Niños accompanied with stronger poleward heat transports?

We have calculated the heat transport the same way as in Sun (2000b). The ocean heat content H_c was first calculated from the ocean temperature data provided by NCEP assimilation for the Pacific Ocean (Ji et al. 1995). Then the heat balance equation of the ocean

$$\frac{\partial}{\partial t}H_C = F_S + D_O, \tag{1}$$

was employed to obtain the convergence of heat in the ocean D_o; and thereby the heat divergence out of the equatorial region ($-D_o$). In Eq. (1) F_s is the surface heat flux into the ocean; F_s was from the NCEP reanalysis (Kalnay et al. 1996). The surface heat flux used in Sun (2000b) and Sun and Trenberth (1998) was derived using ERBE data (Barkstrom et al. 1989) and the energy balance of the atmosphere (Trenberth 1997; Sun and Trenberth 1998; Trenberth et al. 2001), which is only available for the ERBE period. The mean equatorial surface heating from NCEP is somewhat weaker compared with the derived product used in Sun and Trenberth (1998) (Fig. 2). The interannual variability in the NCEP surface heating also appears to be somewhat weaker (Fig. 3). Since the derived product is also subject to error, the differences in the two products at best provide a measure of the potential error in the NCEP surface heating. Note that the main features in the mean and the anomaly agree well between these two products (Figs. 2 and 3). Moreover, as shown in Sun and Trenberth (1998), the interannual variability in F_s is small compared to the interannual variability in H_c and thus the interannual variability in D_o is mainly provided by the interannual variability in H_c. In calculating H_c, the depth of the upper ocean is chosen as 380 m. Below 380 m, there is little variability in the ocean temperature ($<$0.1 K; Sun and Trenberth 1998).

The poleward ocean heat transport out of the equatorial region (5°S–5°N) is presented in Fig. 4. The figure shows that the heat removal from the equatorial Pacific is achieved episodically—active periods with large

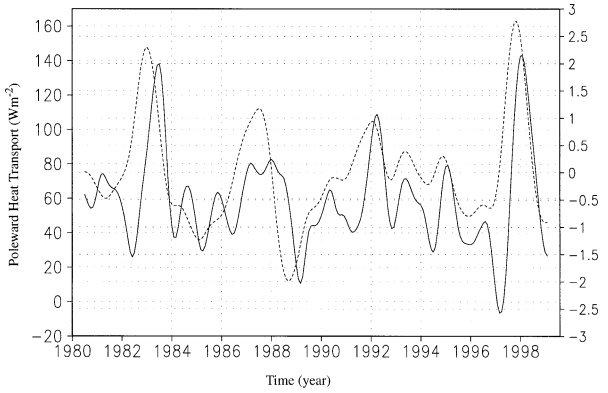

FIG. 5. Poleward ocean heat transport out of the equatorial region (5°S–5°N) with the seasonal variations removed. The seasonal variations were removed by first removing the climatology of 1980–98. The climatological annual mean value was then added to restore the sign of the transport. A Hanning window with a width of 13 months was used to smooth the data. The dashed line indicates Niño-3 SST anomaly.

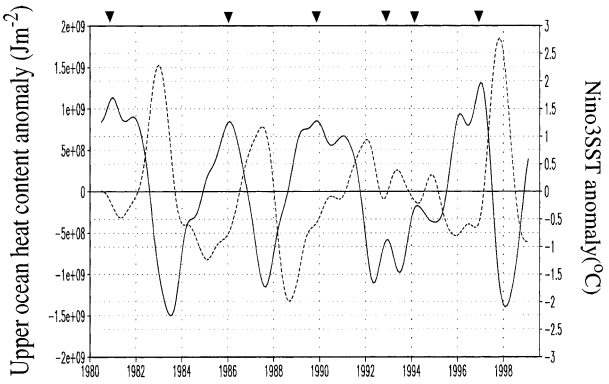

FIG. 6. Time series of the upper-ocean heat content of the western half of the equatorial Pacific (120°–205°E). The time series shown by the dashed line is the SST anomaly of the Niño-3 region. A Hanning window with a width of 13 months was used to smooth the SST and the heat content. The long-term mean value of the heat content was removed. Shown is the ocean heat content above 260 m. Further increasing the depth in calculating the upper-ocean heat content does not change the magnitude of variability significantly, suggesting variability is mostly confined in the upper 260 m. Note that all El Niños are preceded by a peak in the heat content of the western Pacific. The triangles at the top mark the timing of these peaks.

poleward heat transport are preceded and then followed by quiescent periods during which the transport is small. There is significant seasonal variability, but correspondence between the active periods and the observed El Niños is evident. The observed El Niños during this period include 1982/83, 1986/87, 1991/92, 1993, 1994/95, and 1997/98. The correspondence between the active periods and the observed El Niños is more clearly seen when the seasonal variations are removed (Fig. 5). Note that the peak value of the heat transport out of the equatorial Pacific (5°S–5°N) associated with the 1997/98 El Niño almost doubles the mean peak value associated with the four weaker El Niños (1986/87, 1991/92, 1993, and 1994/95). Figure 5 also shows that the peak transport generally lags the peak surface warming in the equatorial Pacific.

These results add further support to the earlier suggestion that El Niño is a major mechanism by which the ocean transports heat from the equatorial ocean to the higher latitudes, just as atmospheric convection is a mechanism to transport heat upward away from the surface.[1] An immediate issue raised by this notion is what the role of La Niña is. As we will see in the next section, the heat removed poleward by El Niño is heat stored in the subsurface ocean of the equatorial western Pacific. La Niña, as we will suggest in section 2c; represents a mechanism to absorb heat from the atmosphere and store the heat in the subsurface ocean of the equatorial western Pacific. Thus, both phases of ENSO play a critical role in the planetary-scale heat transfer in the coupled tropical ocean–atmosphere, though their roles appear to be distinctly different. The notion that El Niño represents a poleward heat removal mechanism also does not contradict the traditional understanding of the role of Ekman transport in the heat balance of the tropical Pacific. As demonstrated by Brady (1994), both the meridional overturning and the gyre transport contribute to the increase in the transport during and immediately after El Niño warming.

b. The heat content in the western Pacific and the magnitude of El Niño warming

All El Niños are preceded by a buildup of heat content in the equatorial western Pacific [defined here as the western half of the Pacific (120°–205°E)]. The 1982/83 and 1997/98 El Niños were preceded by the strongest buildup of heat content in the equatorial western Pacific (Fig. 6). All El Niños are followed by a depletion of heat content in the equatorial western Pacific, reflecting the effect of the anomalous eastward and poleward heat transport during El Niños. Note that the 1982/83 and the 1997/98 El Niños result in the largest drop in the heat content of the equatorial western Pacific. It thus appears that El Niño acts as a regulator of the upper-ocean heat content in the equatorial western Pacific. The larger the buildup of heat in the equatorial western Pacific, the stronger the subsequent El Niño warming

[1] Here it may be useful to note an appealing but false argument concerning the role of ENSO in the heat balance of the tropical Pacific. The argument is that while there is increased ocean heat export from the equatorial region during El Niño, there is also decreased transport during La Niña. Hence the ENSO simply causes interannual variations in the time-mean poleward heat transport. The problem with this argument becomes obvious once one asks the question of how the time-mean poleward heat transport is achieved. Some pioneering models for ENSO, such as the model of Zebiak and Cane (1987), fixed the mean climate to the observed, but the success of these models in simulating ENSO in the present climate does not imply that ENSO does not play a role in maintaining the mean climate.

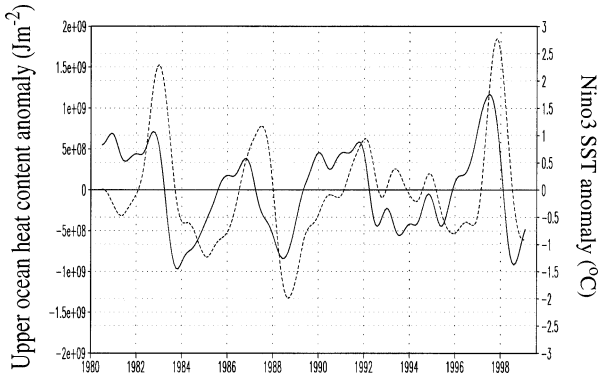

FIG. 7. Time series of the equatorial upper-ocean heat content (120°–290°E). The time series shown by the dashed line is the SST anomaly of the Niño-3 region. A Hanning window with a width of 13 months was used to smooth the SST and the heat content. The long-term mean value of the heat content was removed. Shown is the ocean heat content above 260 m.

which further results in stronger poleward heat transport and thereby a larger drop in the heat content of the western Pacific. The drop in the heat content of the western Pacific is followed by a drop in the heat content in the entire equatorial Pacific (Fig. 7) as the heat is eventually pushed to the higher latitudes, consistent with Fig. 4.

The question is then why El Niño occurs in a way as if it attempts to regulate the long-term heat content in the western Pacific. One possibility is that western Pacific heat content is linked to the stability of the coupled system and El Niño prevents the coupled system from becoming very unstable, consistent with the notion that El Niño results from an instability (Zebiak and Cane 1987; Battisti 1988).[2] Figure 8 supports this interpretation. The figure shows that the higher the heat content in the western Pacific, the stronger the zonal tilt of the thermocline. Thus the heat content in the western Pacific is linked to the potential energy of the equatorial upper ocean and therefore to the stability of the coupled equatorial ocean–atmosphere system.

c. The role of La Niña in the planetary-scale heat transfer in the coupled tropical ocean–atmosphere

The spatial pattern of the heating over the equatorial ocean has a clear correspondence with the main feature of the SST distribution in that region—the equatorial

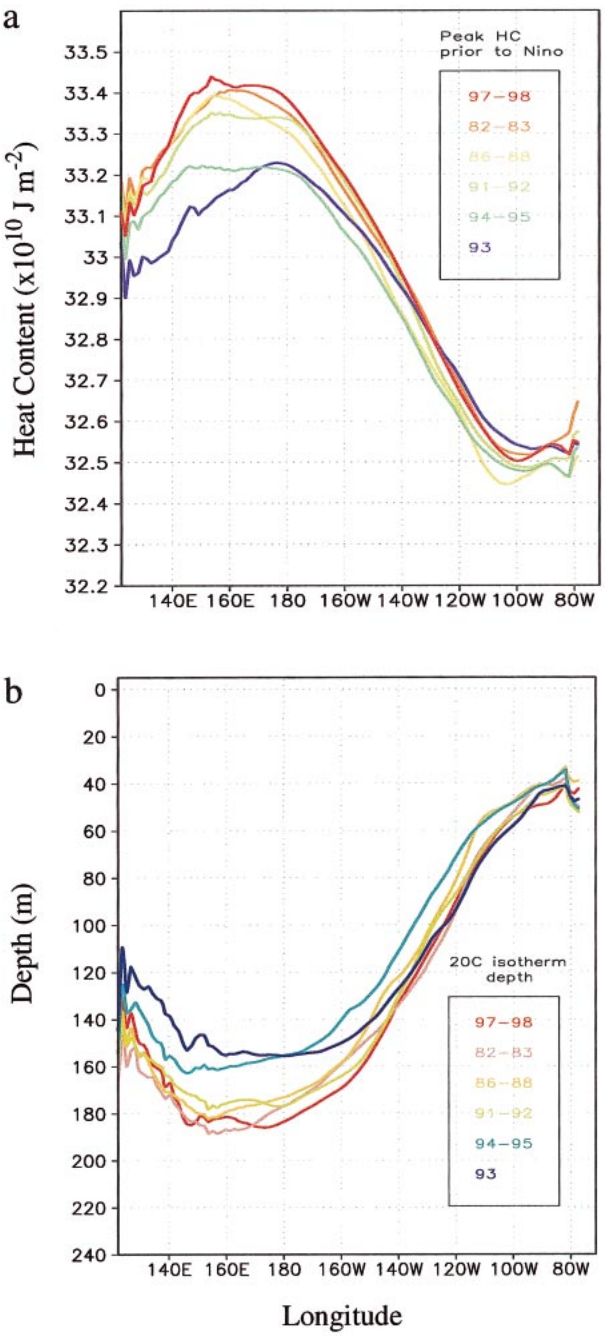

FIG. 8. (a) Zonal distribution of upper-ocean heat content (0–260 m) in the equatorial belt (5°S–5°N) when the western Pacific heat content reaches its pre–El Niño peak. The timing of each pre–El Niño peak is marked by a triangle on Fig. 6. (b) The corresponding depth of the 20°C isotherm. Upper-ocean heat content used for Fig. 8a and the ocean temperature used for calculating the 20°C isotherm depth in Fig. 8b were smoothed in time using a Hanning window with a width of 13 months.

[2] The notion that El Niño results from an instability does not necessarily imply that the observed time-mean state is unstable, just as moist convection in the Tropics resulting from an instability does not necessarily imply that the time-mean thermal structure of the Tropics is convectively unstable. Penland and Sardeshmukh (1995) have suggested that the observed time-mean state of the coupled tropical ocean–atmosphere is probably neutral for coupled disturbances like El Niño. Xu and Emanuel (1989) have suggested that the climatological thermal structure of the tropical atmosphere may not be conditionally unstable for moist convection.

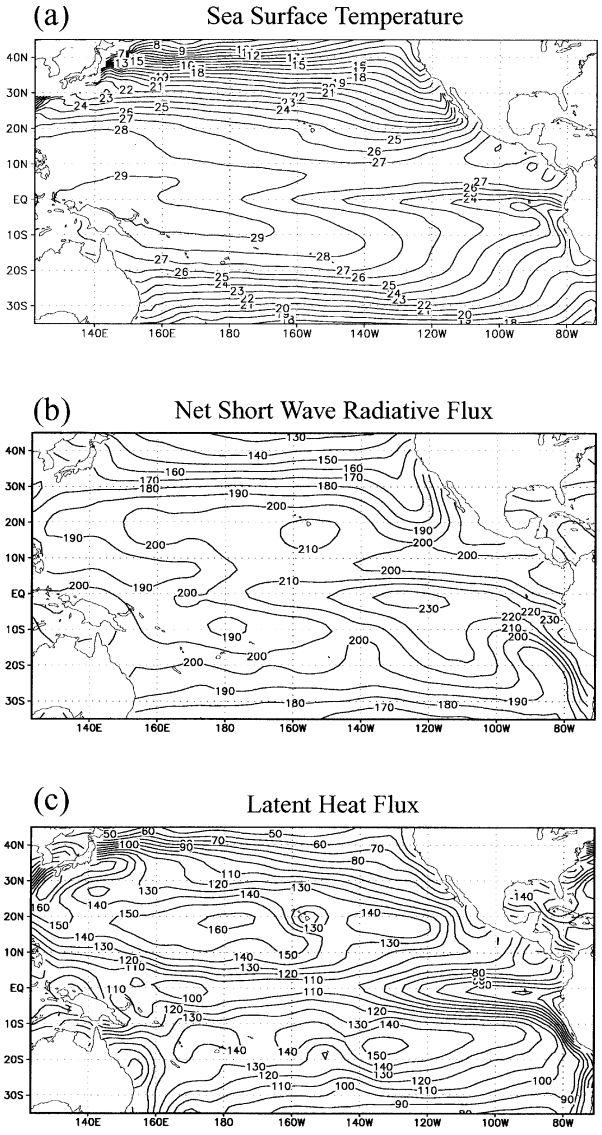

FIG. 9. (a) Annual mean climatological distribution of SST (°C), (b) net downward solar heat flux (W m^{-2}), and (c) latent heat flux (W m^{-2}) over the tropical Pacific. The heat flux data are from the NCEP reanalysis over the ERBE period.

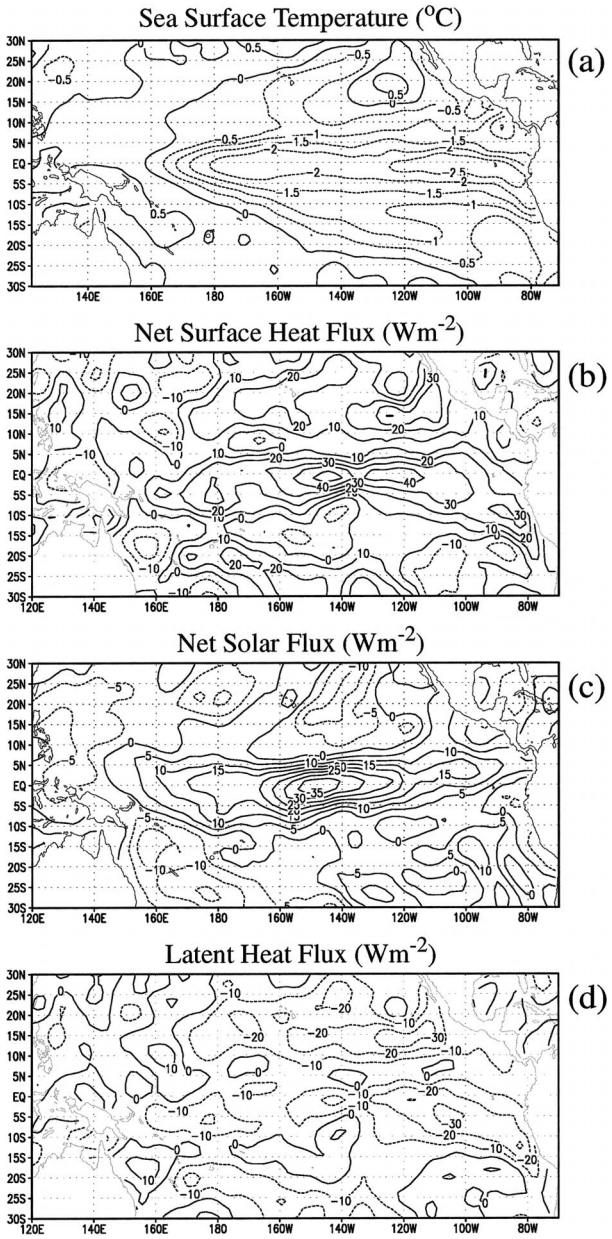

FIG. 10. Differences in (a) SST, (b) net surface heat flux into the ocean, (c) net solar flux into the ocean, and (d) the latent heat flux out of the ocean between 1985 and 1987 (1985 minus 1987). The heat flux data are from the NCEP reanalysis.

cold tongue (Fig. 9a). Figures 9b and 9c display the two main components in the surface energy budget—the net solar radiation and the latent heat flux. The equatorial cold tongue corresponds to a local maximum in the solar flux into the ocean and a local minimum in the latent heat flux out of the ocean. The equatorial cold tongue corresponds to the descending branch of the Walker circulation where deep convection is suppressed and thereby more solar radiation is allowed to reach the ocean's surface. On the other hand, the surface water in that region has a colder SST than the warm pool region, and therefore there is less loss of heat through surface evaporation. Figure 10 further contrasts the differences in SST, net surface heat flux, net solar radiation, and latent heat flux between 1985 and 1987. The year 1985 has a stronger zonal SST contrast than 1987. It also has a much stronger surface flux into the equatorial ocean, apparently because of a larger solar heat flux into the equatorial ocean and a reduced latent heat flux out of the equatorial ocean.

The relationship between the equatorial zonal SST contrast and the net surface heat flux into the equatorial ocean may also be understood from the perspective of the energy balance of the overlying atmosphere. The

equatorial cold tongue corresponds to a region where energy in the atmosphere converges from the surrounding warmer region, the western Pacific warm pool in particular. The colder the cold tongue is relative to the warm pool (i.e., the larger the zonal SST contrast), the more energy converges over the cold tongue region. The net radiative flux at the top of the atmosphere, however, is insensitive to changes in the SST because of the radiative feedbacks of water vapor and clouds, as evident in the ERBE data (Sun 2000b). The consequence is that the stronger the zonal SST contrast, the stronger the surface heat flux into the equatorial ocean (Sun 2000b).

Also note that the stronger the equatorial zonal SST contrast, the stronger the equatorial zonal winds, which push the additional heat absorbed at the surface down into the equatorial upper ocean through tilting and deepening the thermocline (Fig. 11). It thus appears that the equatorial cold tongue and the associated zonal SST contrast represent a mechanism by which heat is sucked into the equatorial upper ocean.

d. The ''heat pump'' hypothesis

The analysis of the heat balance over an extended period confirms that El Niño is a major mechanism by which the tropical Pacific transports heat poleward. More importantly, the analysis shows more clearly that El Niño is a regulator of the heat content in the equatorial western Pacific. In addition, the analysis highlights the positive relationship between the equatorial surface heating, the equatorial zonal SST contrast and hence the magnitude of La Niña, the heat content in the equatorial western Pacific, and the stability of the coupled system. Synthesizing these results, we envision the following scenario concerning how the amplitude of ENSO may respond to an increase in the tropical maximum SST: an increase in the tropical maximum SST initially increases the zonal SST contrast via the dynamical thermostat mechanism of Sun and Liu (1996) and Clement et al. (1996).[3] A stronger zonal SST contrast then strengthens the surface winds and thereby helps the ocean to store more heat to the subsurface ocean. Because of the stronger winds and the resulting steeper tilt of the equatorial thermocline, the coupled system is potentially unstable and is poised to release its energy through a stronger El Niño warming. A stronger El Niño then pushes the accumulated heat poleward and prevents heat buildup in the western Pacific. This scenario will be termed a ''heat pump'' hypothesis for ENSO. It will be investigated in section 3 using a numerical model.

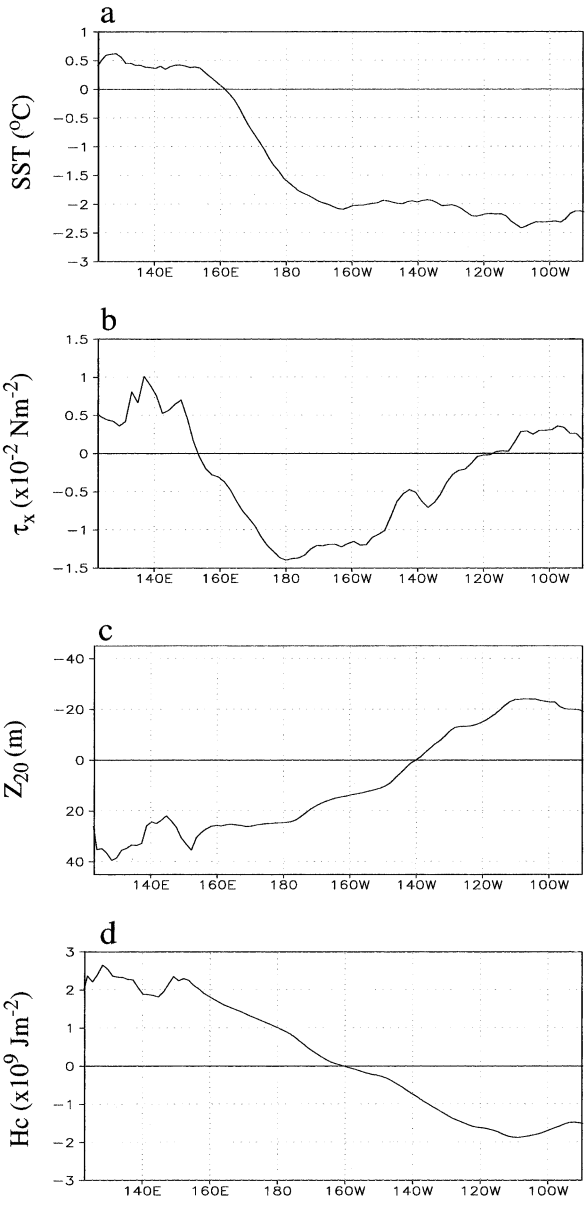

FIG. 11. Differences in equatorial (a) SST, (b) zonal wind stress, (c) slope of the thermocline measured by the depth of the 20°C isotherm, and (d) the upper-ocean heat content between 1985 and 1987 (1985 minus 1987). The data for the zonal wind stress are from the NCEP reanalysis.

3. Numerical results

a. The model

We choose the NCAR CSM Pacific Basin model—the model of Gent and Cane (1989)—as our ocean component. In contrast to the intermediate model of the type of Zebiak and Cane (1987) in which only the heat budget

[3] As found by Sun and Liu (1996) and Clement et al. (1996), an initially zonally uniform increase in the surface heating results in a stronger zonal SST contrast because the effect of heating is opposed more in the eastern equatorial Pacific by the upwelling, but less so in the western Pacific because of the preexisting zonal asymmetry in the distribution of upwelling.

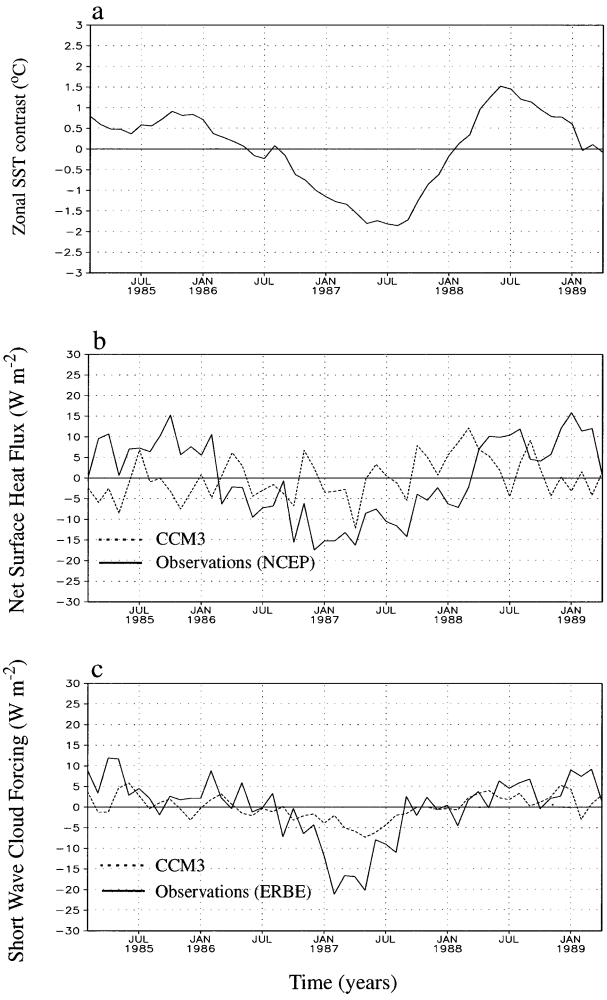

FIG. 12. (a) Variations of the zonal SST contrast across the equatorial Pacific over the ERBE period. The equatorial zonal SST contrast is measured by the area-averaged SST differences between (5°S–5°N, 130°–180°E) and (5°S–5°N, 230°–280°E). (b) Variations in the net surface heat flux over the equatorial Pacific (5°S–5°N, 120°–290°E) from CCM3 (dashed line) and from the NCEP reanalysis (solid line). (c) Variations in the shortwave cloud forcing over the equatorial Pacific (5°S–5°N, 120°–290°E) from CCM3 (dashed line) and from ERBE observations (solid line). All quantities shown are their interannual anomalies.

of the mixed layer is explicitly calculated, the model of Gent and Cane (1989) explicitly calculates the heat budget of the entire upper ocean. For our present purpose, which is to examine how the coupled ENSO system responds to an increase in the surface heating, it is crucially important to explicitly calculate the heat budget of the entire upper ocean. The domain of the Pacific Basin model is 30°S–30°N and 123°–289°E. Its spatial resolution in the longitudinal direction is 1° and has variable resolution in the latitudinal direction. Within the equatorial waveguide, the resolution is very fine (about 0.25°) and therefore ensures accurate simulation of the equatorial waves.

In assessing whether NCAR's Community Climate Model version 3 (CCM3; Kiehl et al. 1998) is suitable for our purpose, we have noted that CCM3 does not simulate correctly the relationship between the surface heat flux and the zonal SST contrast. Figure 12a shows variations of the observed equatorial zonal SST contrast over the ERBE period (February 1985–April 1989). Figure 12b shows the corresponding variations of the net surface heat flux into the equatorial ocean from observations and a CCM3 run with the observed SST (Kiehl et al. 1998). Observations show that as the zonal SST strengthens and weakens, the net surface heat flux increases and decreases accordingly. Such a relationship is barely evident in the CCM3 simulation. This inadequacy in simulating the relationship between the zonal SST contrast and the net surface heat flux is apparently linked to a problem in the representation of cloud feedbacks. Figure 12c compares the variations of shortwave cloud forcing over the ERBE period from observations and CCM3. Observations show that in response to surface warming during El Niño, more clouds develop to shield the solar radiation from reaching the ocean's surface. The CCM3 simulation barely captures this effect. As noted by Cess et al. (1990), cloud feedbacks are also not well simulated in many other GCMs.

The above analysis helps to illustrate an important, but often overlooked point, which is that while the overall capability of a comprehensive GCM may be better than a simpler or more empirically based climate model, it is not necessarily closer to nature in every aspect than the simpler models. In view of the problems that CCM3 has with clouds, we take a more empirical approach here. The net surface heat flux into the ocean is assumed to be proportional to the differences between the actual SST and the potential SST—the SST the ocean would have if it acted as a mixed layer without any heat transport,

$$F_s = C_p \rho c H_m [\mathrm{SST}_p(\varphi) - \mathrm{SST}(\lambda, \varphi)], \qquad (2)$$

where F_s is the net surface heat flux into the ocean, C_p is the specific heat, ρ is the density of water, c is the restoring coefficient, H_m is the depth of the mixed layer which has a fixed value in the ocean model (50 m), φ is the latitude, and λ is the longitude. Considering the energy balance of the overlying atmosphere,

$$F_s = N_T + D_a = S_c - E + G_a + C_l + C_s + D_a, \qquad (3)$$

where N_T is the net radiative flux at the top of the atmosphere, D_a is the horizontal convergence of total energy in the atmosphere, S_c is the clear sky solar radiation, E is the surface emission, G_a is the greenhouse effect of water vapor, C_l is the greenhouse effect of clouds, and C_s is the shortwave forcing of clouds, the restoring coefficient may be linked to atmospheric feedbacks by

$$c = \frac{1}{C_p \rho H_m}\left(\frac{\partial E}{\partial \mathrm{SST}} - \frac{\partial D_a}{\partial \mathrm{SST}} - \frac{\partial G_a}{\partial \mathrm{SST}} - \frac{\partial C_l}{\partial \mathrm{SST}} - \frac{\partial C_s}{\partial \mathrm{SST}}\right). \qquad (4)$$

Using the values provided by Sun and Trenberth (1998), c is estimated to be 5.8×10^{-8} s^{-1}, corresponding to a relaxation time of 200 days. Equation (2) has been used frequently in earlier theoretical studies (Neelin et al. 1998; Sun and Liu 1996; Clement et al. 1996). The resulting relationship between the surface heat flux and SST on the interannual timescale is supported by recent observational results (Sun and Trenberth 1998; Trenberth et al. 2001).

In reference to the observed SST and the net surface heat flux from the NCEP reanalysis, SST_p is assumed to take the following form:

$$SST_p = A + B \cos\left(\frac{\varphi}{30}\pi\right), \quad (5)$$

where A and B are empirical constants.

Over the equatorial western Pacific warm pool, F_s has to be very small (Gent 1991). Therefore, by Eq. (2), the SST in the equatorial western Pacific warm pool must be very close to SST_p. This further implies a positive relationship between the net surface heat flux into the equatorial ocean and the equatorial zonal SST contrast, consistent with observations. This formulation is also consistent with some earlier theoretical studies of ENSO in which SST_p was termed the SST of the radiative–convective equilibrium state of the coupled system (Neelin 1991; Neelin and Jin 1993; Sun and Liu 1996; Sun 1997). Also in line with these earlier theoretical studies, the zonal equatorial wind stress (5°S–5°N) is coupled to the equatorial zonal SST contrast,

$$\tau^x = \tau^x_{\text{ref}} - \mu(\Delta T - \Delta T_{\text{ref}}), \quad (6)$$

where τ^x is the actual zonal wind stress in the equatorial region (5°S–5°N), τ_{ref} is the corresponding value of a reference state, ΔT and ΔT_{ref} measure, respectively, the equatorial zonal SST contrast of the actual and the reference state, and μ is a parameter that measures the sensitivity of surface wind stress to changes in the equatorial zonal SST gradients. The coupling of the zonal wind stress with the zonal SST contrast is assumed to decrease away from the equatorial region following a cosine profile. Outside the region of 15°S–15°N, the influence of changes in the equatorial zonal SST contrast on winds is assumed to be negligible. As argued in earlier theoretical studies of ENSO, the effect of the meridional wind stress anomaly on the coupled equatorial wave dynamics is secondary, and therefore for the first-order approximation, the feedback from the meridional wind stress may be neglected.

b. Numerical results

To test the ''heat pump'' hypothesis inferred from observations, two experiments with this coupled model have been carried out. Experiment II (warm case) differs from experiment I (cold case) only in $SST_p(\varphi)$ and the difference is confined to the equatorial region (5°S–5°N). [The difference in $SST_p(\varphi)$ follows a cosine profile with a value of 2 K at the equator and zero at the edge of 5°S–5°N.] The annual mean wind stress from the NCEP reanalysis for the period of 1980–99 was used as the wind stress of the reference state (τ^x_{ref}) (Fig. 13a). The SST of the reference state was obtained by spinning up the ocean model to equilibrium with this wind stress forcing and a specified profile of $SST_p(\varphi)$ in the form of Eq. (3) ($A = 26$°C, $B = 5$°C). The resulting equilibrium SST is shown in Fig. 13b. Note that the reference state is an equilibrium solution of the coupled model. The equatorial zonal SST contrast in Eq. (6) is measured by the area-averaged SST differences between (5°S–5°N, 130°–180°E) and (5°S–5°N, 230°–280°E). In reference to the interannual variations of the equatorial zonal wind stress over the central equatorial Pacific and the corresponding interannual variations in the equatorial zonal SST contrast from NCEP reanalysis, a value of 0.0060 N m^{-2} K^{-1} is used for parameter μ. Instantaneous coupling was used to obtain the results from the coupled model shown here—fluxes of heat and momentum were computed every ocean time step. We have

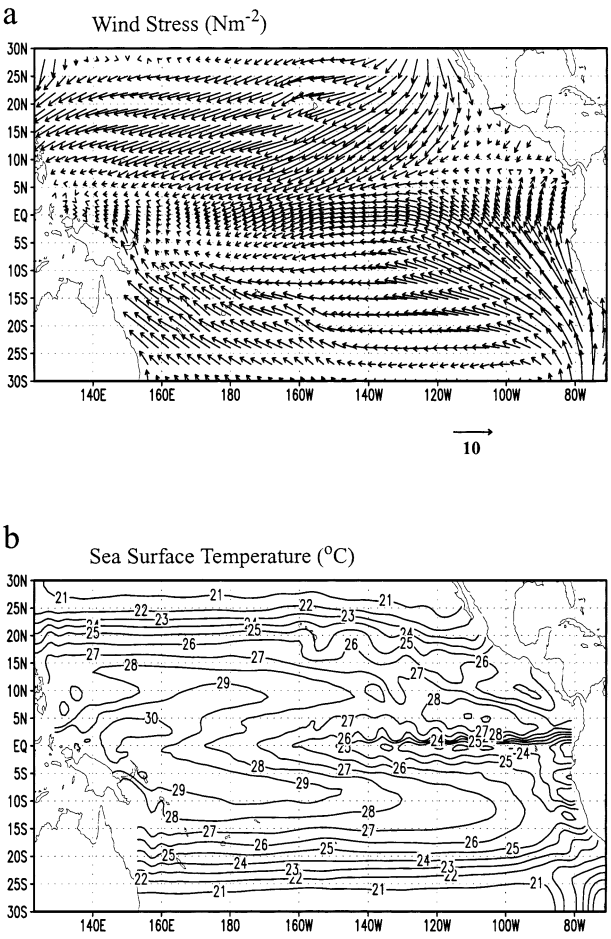

FIG. 13. The (a) wind stress and (b) SST of the reference state. See text for more details.

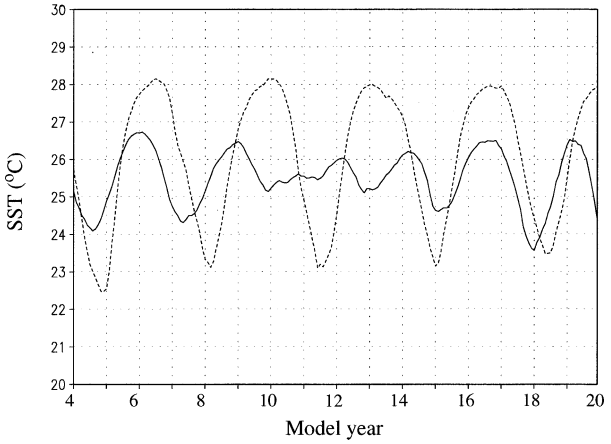

FIG. 14. Time series of Niño-3 SST from experiment I (solid line) and experiment II (dashed line). Experiment II starts with the same initial conditions as experiment I, and both are run for 20 yr. Shown are the last 16 yr of the experiments. Experiment II has a higher $SST_p(\varphi)$ than experiment I in the equatorial region.

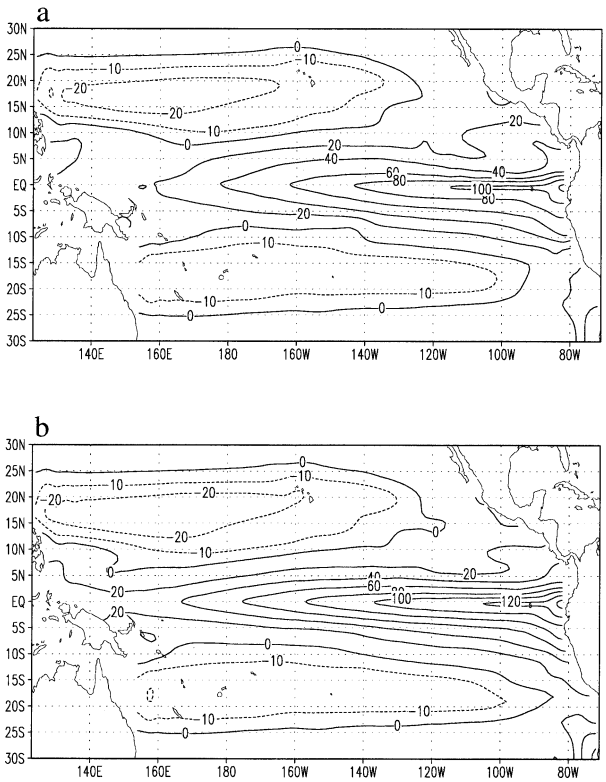

FIG. 15. Long-term mean surface heat flux (W m^{-2}) in (a) experiment I and (b) experiment II.

further found that switching to the use of 10-day average in calculating the interfacial fluxes leads to very similar results.

Figure 14 shows Niño-3 (5°S–5°N, 90°–150°W) SST variations from experiment I and experiment II. The corresponding time-mean distributions of surface heating are shown in Fig. 15. Consistent with observations, the distribution of surface heating in these two runs is characterized by heating in the equatorial region and cooling in the subtropics. Both experiments have self-sustained oscillations. The oscillation has a period of 3–4 yr, which is consistent with observations and with the results from the intermediate model of Zebiak and Cane (1987). Also consistent with observations, the warming is confined to the equatorial central and eastern Pacific (Fig. 16). The evolution of the subsurface ocean temperature over the life cycle of the model El Niño closely follows observations (Fig. 17). The initiating stage is characterized by a warm anomaly in the western Pacific. The warm anomaly extends to the east following the undercurrent, which characterizes the development stage. The mature stage is characterized by a zonal redistribution of warm water. The aftermath stage is when the warm water in the upper ocean is depleted.

The oscillations in the case with a stronger equatorial heating are more energetic. Interestingly, while the warm phase becomes warmer, the cold phase also becomes colder. The colder temperature in the cold phase in the eastern equatorial Pacific is apparently due to the ''dynamical thermostat'' mechanism of Sun and Liu (1996) and Clement et al. (1996). The zonal SST contrast during the cold phase is much enhanced during the cold phase in experiment II (Fig. 18a). The resulting stronger winds then enhance the zonal slope of the thermocline—the thermocline in the west equatorial Pacific deepens while the thermocline in the east becomes shallower (Fig. 18b). A shallower thermocline in the eastern equatorial Pacific implies that the temperature of the subsurface water upwelling into the surface layer of that region is colder. So any initial increase in the zonal SST contrast will be enhanced through the positive feedback loop among the SST, the surface winds, and the upper-ocean dynamics. Also noted by Sun and Liu (1996) and Clement et al. (1996), an initially zonally uniform increase in the surface heating is opposed in the eastern equatorial Pacific by the upwelling, but less so in the western Pacific because of the preexisting zonal asymmetry in the distribution of upwelling.

The dynamical thermostat mechanism of Sun and Liu (1996) and Clement et al. (1996), however, is a fitting prediction only for the response of the zonal SST contrast during the cold phase. Averaged over the entire life cycle of ENSO, the zonal SST contrast is only slightly larger in experiment II than in experiment I (Fig. 19a). The increase in the time-mean zonal SST contrast from experiment I to experiment II is less than 10% (0.4°C). In contrast, the variance of the Niño-3 SST in experiment II is more than twice as large as in experiment I. Thus the zonal SST contrast may be regarded as insensitive to increases in the surface heating. This is because El Niño—the warm phase of the oscillation—warms the eastern Pacific and cools the western Pacific (Fig. 19b). Note that despite a 2-K increase in SST_p in experiment II, the SST in the far western equatorial Pacific changed little in the warm phase, indicating a

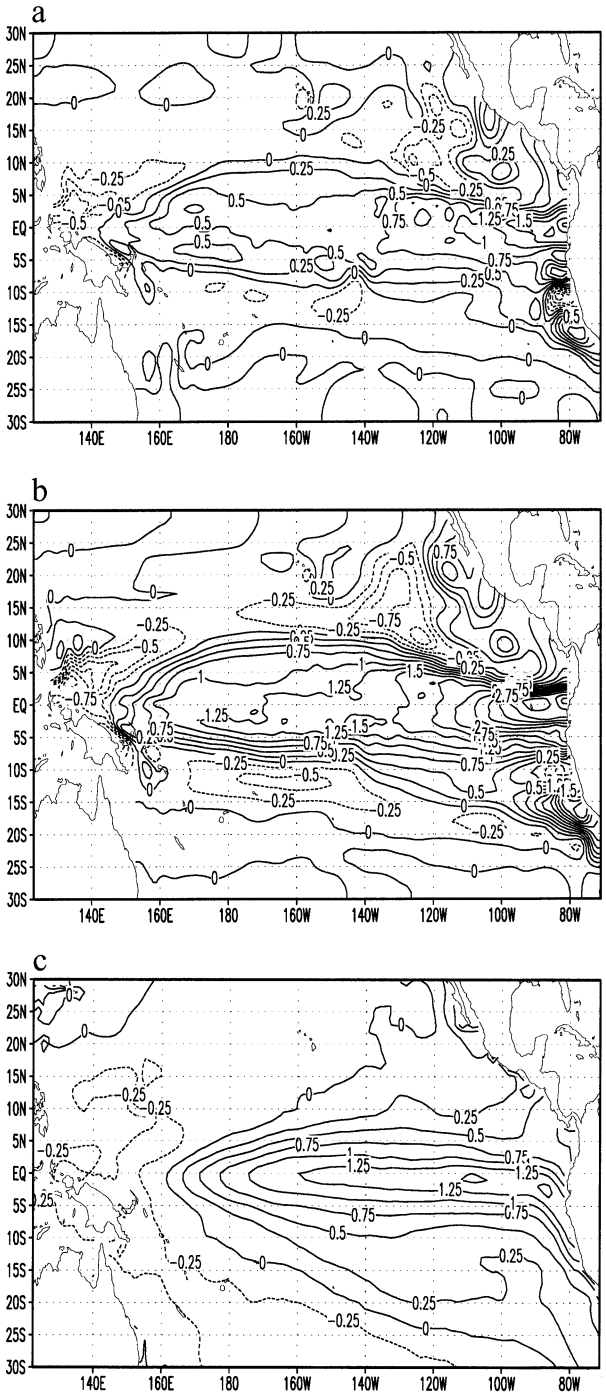

FIG. 16. SST anomaly (°C) during the warm phase from (a) experiment I, (b) experiment II, and (c) observations. The warm phase starts at the point when the surface warming over the Niño-3 region reaches half of the maximum warming and ends at the point when the surface warming in that region falls to half of the maximum warming. Conversely, the cold phase starts at the time when the cooling already reaches half of the maximum cooling and ends when the cooling recedes to half of the maximum cooling. Shown are composites. For the model experiment, four warm/cold events are used for the composite. The ocean temperature data from the NCEP assimilation system (Ji et al. 1995) are used to construct the composite for the observations and it includes all six El Niños in the last 20 yr.

substantial cooling effect by a stronger El Niño warming on the western Pacific SST. In a sense, El Niño regulates the zonal SST contrast. Sun and Liu (1996) overlooked the cooling effect of El Niño because the model they employed does not have full ENSO dynamics. Clement et al. (1996), on the other hand, used an intermediate ocean model that only has a heat budget for the mixed layer. It is possible that an intermediate ocean model may underestimate the feedback from El Niño on the time-mean climate.

Figure 20 shows the variations in the poleward heat transport away from the equatorial Pacific. The poleward heat transport in experiment II becomes more episodic in the sense that the poleward heat transport is more concentrated in the active period. Consistent with observations and the results of Brady (1994), the maximum poleward heat transport lags the maximum surface warming.

Figure 21a shows the time-mean temperature differences in the upper ocean between experiment I and experiment II. In the upper 200 m, the vertical stratification in the western Pacific slightly decreases from experiment I to experiment II while the vertical stratification in the central and eastern Pacific remains approximately the same. The lack of significant increases in the ''sharpness'' of the time-mean thermocline suggests that the amplitude of ENSO can increase considerably even in the absence of significant increases in the strength of the thermocline. Timmermann et al. (1999), Meehl et al. (2001), and Otto-Bliesner and Brady (2001) recently attributed increases in the amplitude of ENSO in their experiments to a stronger time-mean thermocline. The present results support more the inference from observations that the amount of heat accumulated in the upper ocean of the western and central Pacific during the cold phase is a key element in determining the magnitude of El Niño warming (Fig. 21b). The present experiments further suggest that the amount of heat in the equatorial western Pacific in the cold phase may be proportional to the tropical maximum SST or the intensity of the equatorial surface heating.

The lack of considerable changes in the time-mean upper-ocean thermal stratification results from large cancellations between the corresponding changes in the cold phase and those in the warm phase (Figs. 21a–c). Conversely, if one attempts to search for changes in the time-mean state as candidates responsible for changes in the amplitude of ENSO, one finds that the amplitude of ENSO is very sensitive to changes in the time-mean state, in particular in those aspects that vary widely with ENSO (such as the zonal SST contrast and the vertical stratification in the upper ocean). Latif et al. (1993) noted in their GCM experiments that the amplitude of ENSO is very sensitive to changes in the time-mean state. The present results suggest a possible explanation. Figure 21 also supports strongly the notion that El Niño acts as a regulator of the equatorial upper-ocean heat

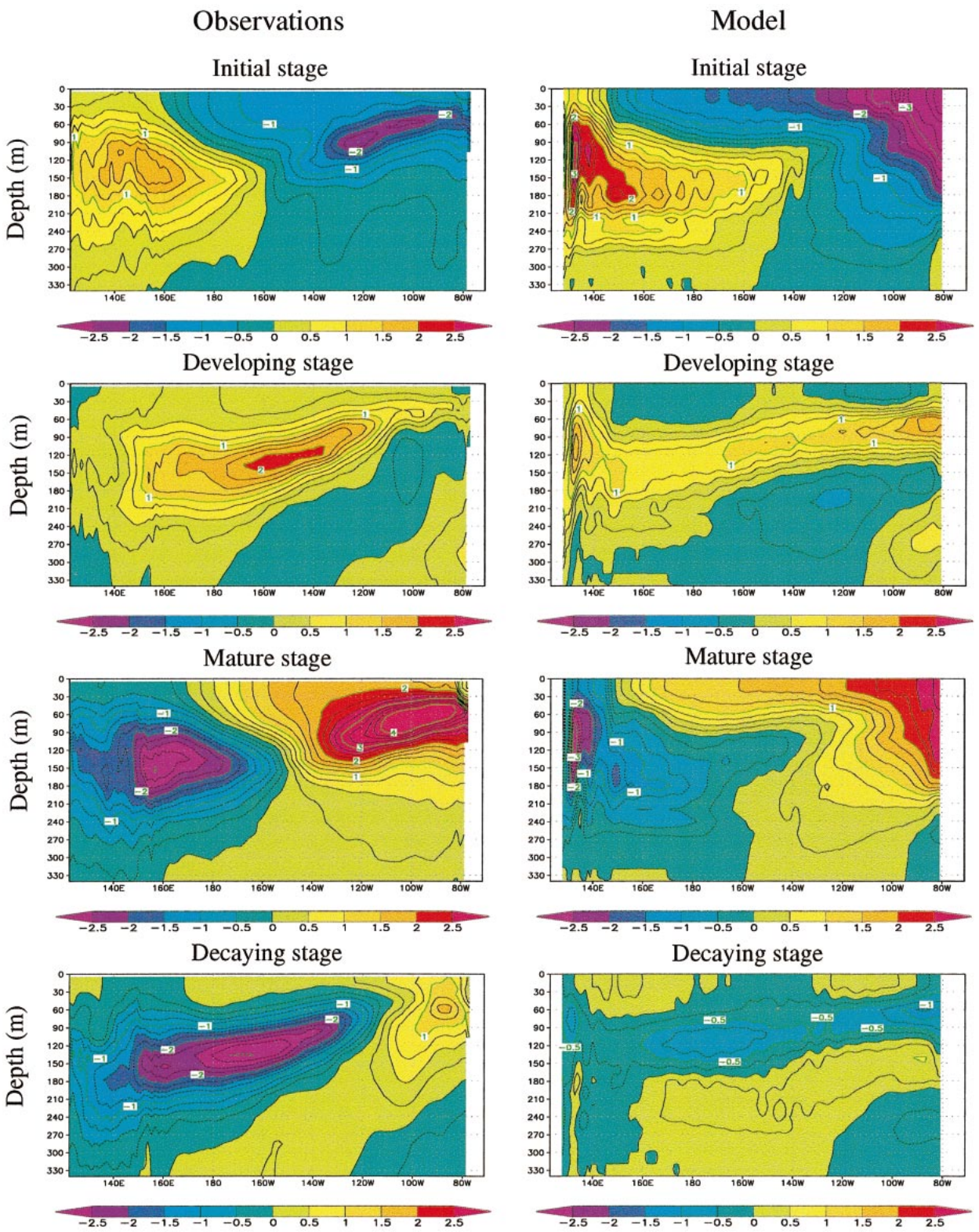

FIG. 17. Evolution of the subsurface temperature at various stages of El Niño from experiment II and observations. The initial state corresponds to the time when the Niño-3 SST anomaly is at a minimum, the developing stage corresponds to the time when the Niño-3 SST anomaly rises to zero, the mature stage corresponds to the time when the Niño-3 SST reaches a maximum, and the decaying stage corresponds to the time when the Niño-3 SST anomaly falls back to zero again. Shown are composites. The composite for experiment II includes four cycles of the model oscillation. The ocean temperature data from the NCEP assimilation system (Ji et al. 1995) are used to construct the composite for the observations and it includes all six El Niños in the last 20 yr.

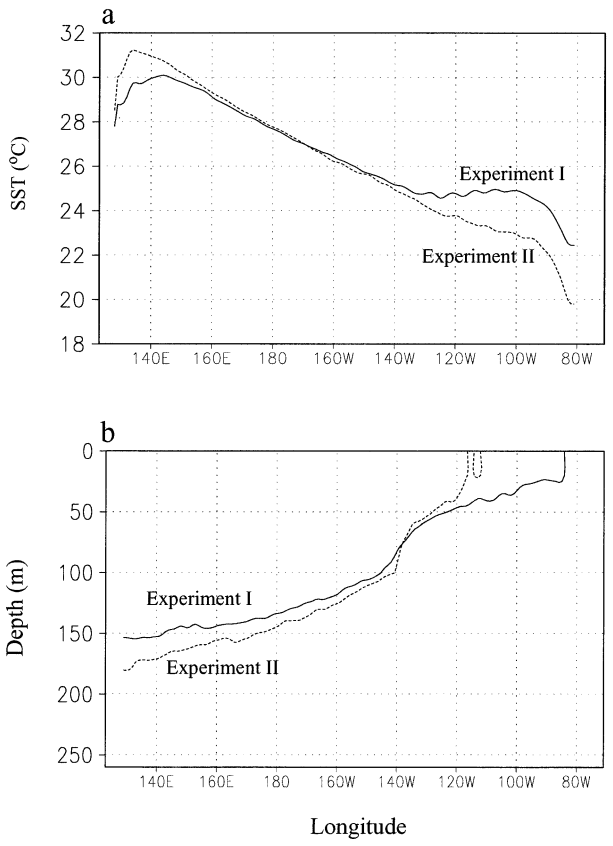

FIG. 18. (a) Zonal distribution of equatorial SST (5°S–5°N) during the cold phase from experiment I (solid line) and experiment II (dashed line). (b) Depth of the 20°C isotherm at the equator during the cold phase from experiment I (solid line) and experiment II (dashed line).

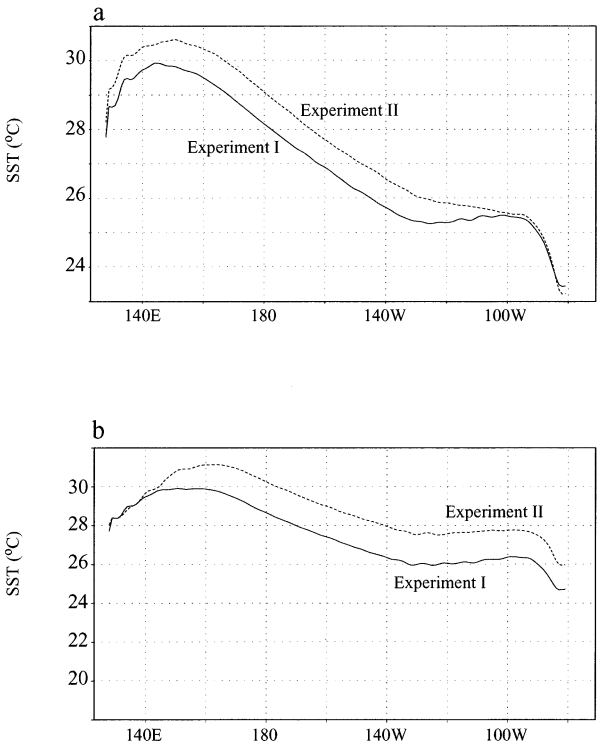

FIG. 19. (a) Zonal distribution of the time-mean equatorial SST from experiment I (solid line) and experiment II (dashed line). The time-mean change in the zonal SST contrast from experiment I to experiment II, measured by the area-averaged SST differences between (5°S–5°N, 130°–180°E) and (5°S–5°N, 230°–280°E), is only about 0.4°C, less than 10% of the time-mean zonal SST contrast in experiment I. (b) Zonal distribution of equatorial SST (5°S–5°N) during the warm phase from experiment I (solid line) and experiment II (dashed line).

content—the heat content in the equatorial western Pacific in particular.

Though the present experiments suggest that the amplitude of ENSO can increase without increases in the strength of the time-mean thermocline, the availability of a source for cold water remains important in the present experiments. Figure 21b indicates that the subsurface water upwelling in the eastern Pacific is colder. Recall that the additional heating introduced in experiment II is confined to the equatorial region. Also note that the deep ocean temperature is kept the same in the two experiments. Thus in the present model, through advection and diffusion, both the equatorial deep ocean and the higher-latitude ocean may be an important source of cold water. Strictly speaking, the key attribute is not the absolute value of the warm-pool SST, but the degree of contrast between the warm-pool SST and the temperature of the water feeding the upwelling in the eastern equatorial Pacific. Studies have suggested that subsurface water that feeds the equatorial upwelling may partially come from higher latitudes (Lu et al. 1998; Liu et al. 1994; McCreary and Lu 1994). Future experiments may need to explore how changes in the subtropical SST or the temperature of the deep ocean may affect the equatorial subsurface temperature and the amplitude of ENSO.

4. Summary and discussion

To better understand the relationship with the tropical maximum SST and the amplitude of ENSO, the heat

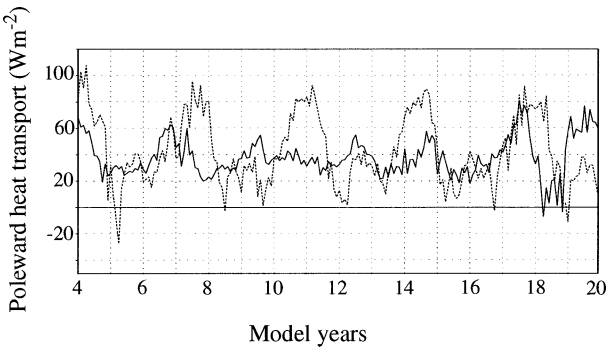

FIG. 20. Time series of the poleward heat transport out of the equatorial Pacific (5°S–5°N) from experiment I (solid line) and experiment II (dashed line).

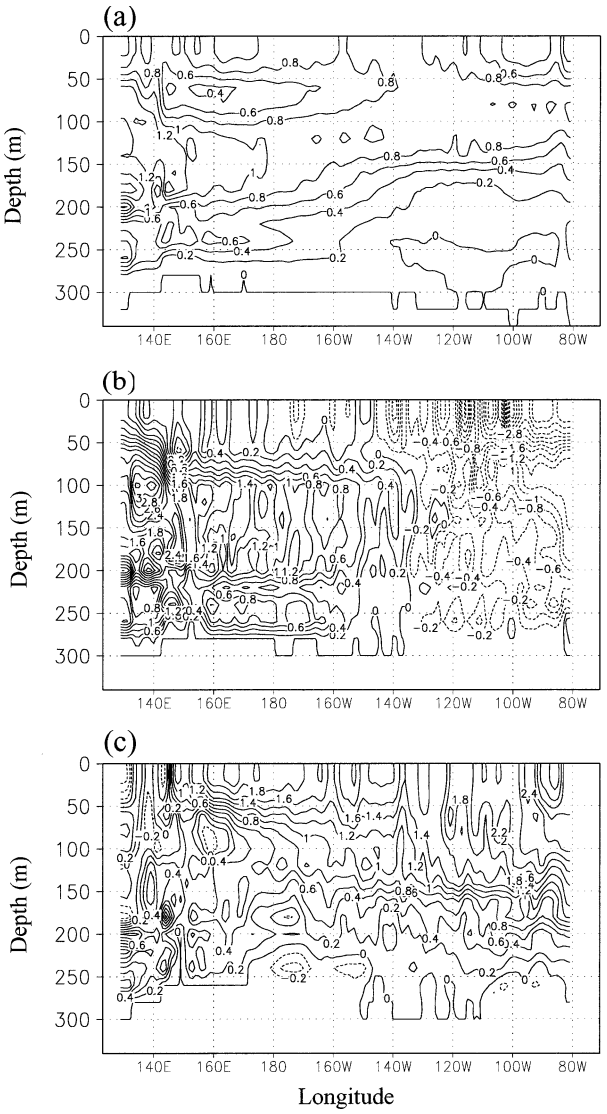

FIG. 21. Upper-ocean temperature differences between experiment I and experiment II (°C) in (a) the time mean, (b) during the cold phase, and (c) during the warm phase. The definitions of the warm and cold phases are the same as in Fig. 16.

balance of the tropical Pacific over the last two decades was first examined. The results suggest that an increase in the tropical maximum SST may result in more energetic El Niños. Numerical experiments with a coupled model in which the ocean component is a GCM and therefore explicitly calculates the heat budget of the entire upper ocean support this suggestion. Increasing the warm-pool SST through increasing the potential SST over the equatorial Pacific initially results in a stronger zonal SST contrast or a stronger La Niña, apparently through the dynamical thermostat mechanism of Sun and Liu (1996) and Clement et al. (1996), which helps the ocean to store more heat in the western Pacific subsurface ocean. A stronger El Niño then develops and pushes the heat poleward with a stronger El Niño warming. These findings are schematically summarized in Fig. 22. The results link the tropical maximum SST, the surface heating, the western Pacific heat content, and the stability of the coupled system. They suggest that the western Pacific heat content may be a key parameter in determining the stability of the coupled system, and that by regulating the heat content in the western Pacific, El Niño may be a mechanism to prevent the coupled system from becoming substantially unstable. Conversely, the processes that maintain a sufficiently high warm-pool SST (relative to the temperature of the subsurface water feeding the upwelling in the equatorial eastern Pacific) are also the processes that keep the ENSO cycle going. We call this extended understanding of El Niño warming a ''heat pump'' picture for ENSO.

The heat pump picture for ENSO advances our understanding of ENSO on two fronts. First, it delineates the importance of a fundamental thermodynamic condition that is required to support El Niño. The picture implies that the existence and strength of ENSO in the present climate owes not only to coupled wave dynamics, but also to a warm-pool SST that is sufficiently high relative to the temperature of the deep ocean. Second, the heat pump picture suggests that the background state—the time mean state—may in turn be determined by ENSO. Specifically, El Niño may regulate the warm pool SST and the associated zonal SST contrast in the time-mean state. Therefore, the heat pump picture ties El Niño to the heat balance of the tropical Pacific. This picture does not reject, but extends the ''delayed oscillator hypothesis'' (Battisti 1988; Suarez and Schopf 1988) or the later ''recharge oscillator'' hypothesis (Jin 1997a,b; Neelin et al. 1998). Note that both the delayed oscillator hypothesis and the later recharge oscillator hypothesis are derived from an anomaly model of ENSO—the intermediate coupled model of Zebiak and Cane (1987). Such a model examines the behavior of a SST anomaly in a fixed environment—the observed time-mean climate (Zebiak and Cane 1987; Neelin et al. 1998). Moreover, despite the recognition that the surface warming is fed by the heat from the subsurface, an anomaly model for ENSO does not have a heat budget for the subsurface ocean. To obtain a realistically looking growth rate and a finite peak amplitude of the surface warming, an anomaly model for ENSO has to further prescribe a relationship between the temperature of the upwelling water and the dynamical depth of the thermocline. Such a prescription further involves the use of a particular reference profile for the vertical structure of the subsurface temperature (Battisti 1988; Jin 1997a,b). While these empirical treatments have allowed a clear delineation of the mechanism for the phase transition of ENSO, they also appear to have obscured the role of the warm pool SST and the associated heat balance of the entire equatorial upper ocean. The present study brings the importance of the heat balance to the forefront and highlights the possibility that El Niño events and the time-mean climate are mutually depen-

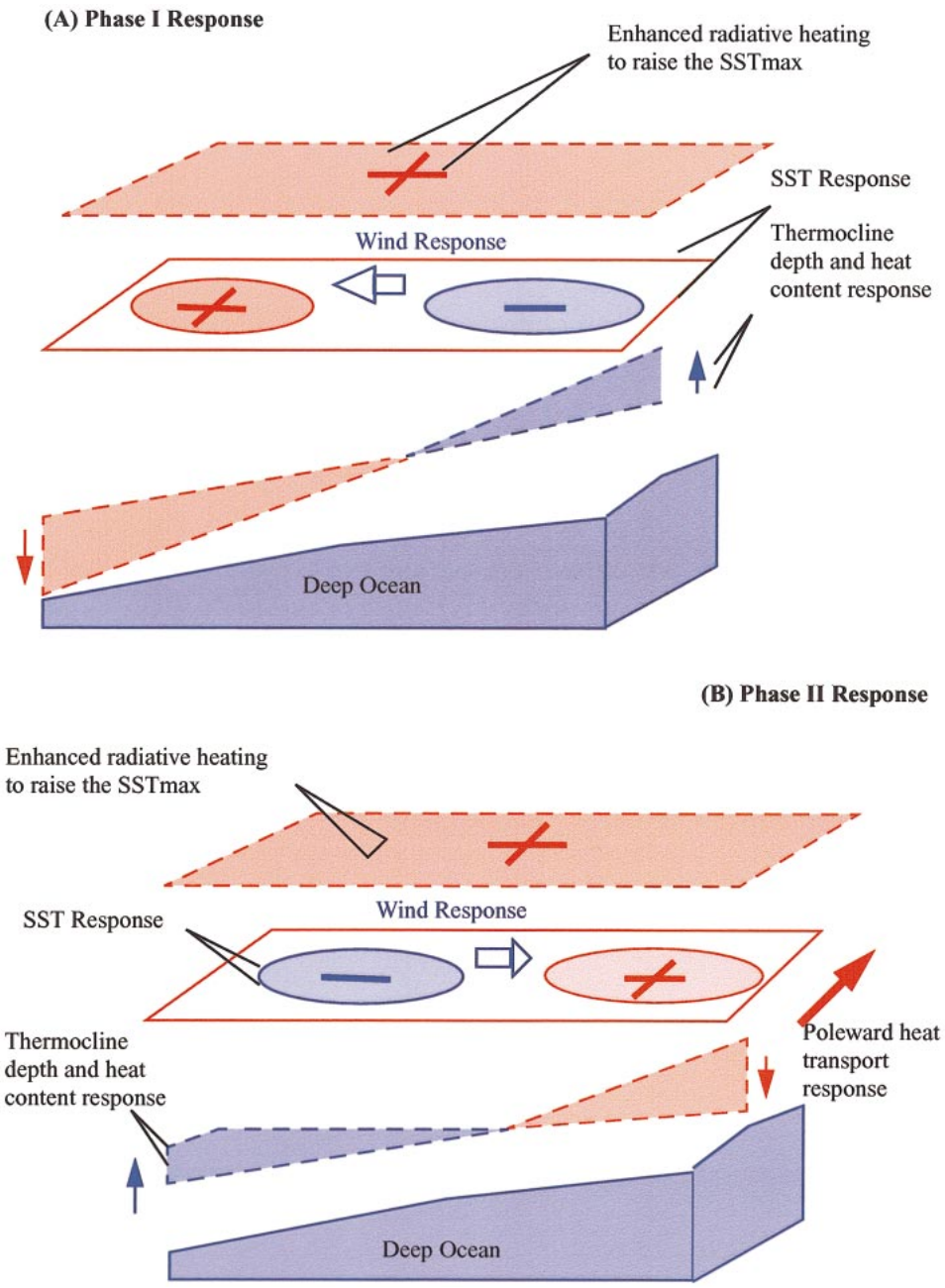

FIG. 22. A schematic showing the heat pump hypothesis for ENSO. The response of the equatorial coupled ocean–atmosphere to an increase in the radiative heating consists of two phases. In phase I, the zonal SST contrast strengthens—the western Pacific becomes warmer but the eastern Pacific becomes colder. This allows the ocean to absorb the added heat from above and transport it to the subsurface ocean—the western Pacific subsurface ocean in particular (Fig. 22a). As the thermocline deepens in the west, however, the ocean becomes more unstable. A stronger El Niño then develops, transporting more heat poleward, reversing the effect of the enhanced radiative heating on the SST and the depth of the thermocline in phase I (Fig. 22b), and thereby minimizing the effect of the enhanced radiative heating on the time-mean structure of the coupled equatorial ocean–atmosphere system.

dent. In an analogy with biology, the coupled wave dynamics emphasized in the delayed oscillator hypothesis (or the delay mechanism underscored in the recharge oscillator hypothesis) may be regarded as a ''gene'' of the coupled climate system. Whether the gene in a real biological organism expresses or fully expresses itself depends on the environment it is subjected to (e.g., whether the environment has sufficient nutrients).

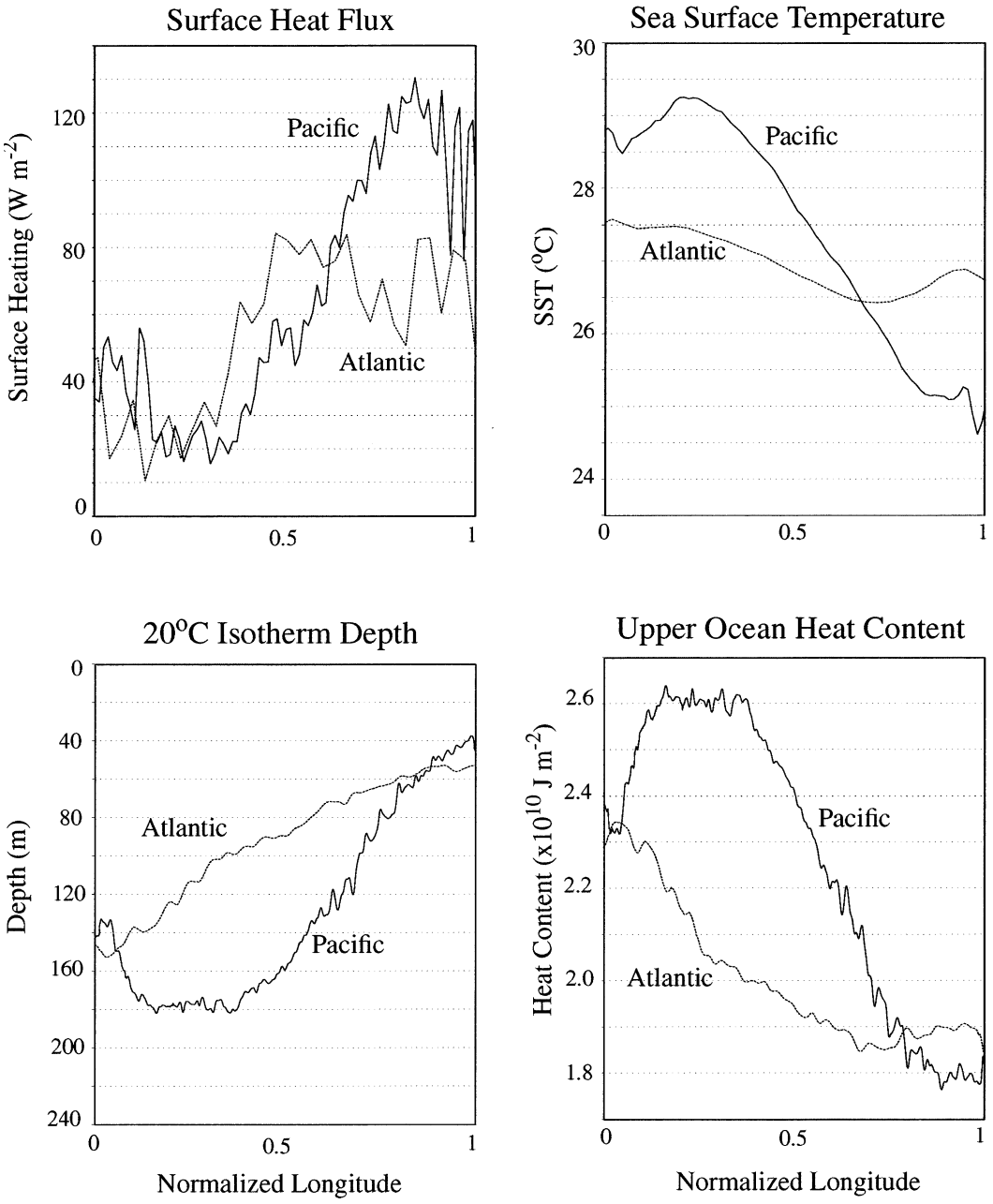

FIG. 23. Comparison of (a) surface heat flux, (b) SST, (c) slope of the thermocline (depth of the 20°C isotherm), and (d) the equatorial upper-ocean heat content (0–260 m) between the equatorial Pacific and the equatorial Atlantic. The normalized longitude is defined as $x^* = (x - x_1)/(x_2 - x_1)$ where x_1 and x_2 are, respectively, the physical longitude that defines the eastern end and western end of the basin (120° and 290°E for the equatorial Pacific, and 310° and 10°E for the equatorial Atlantic). The surface heat flux data used here are the same as that for Fig. 2a. The ocean temperature data are from the Levitus and Boyer (1994) *World Ocean Atlas 1994.*

Whether the coupled climate system is able to sustain El Niño depends on the value of the tropical maximum SST or more simply on how warm the Tropics are relative to the deep ocean. Just as biological organisms may modify their environment, how warm the Tropics are may in return depend on the magnitude of El Niño events. The heat pump picture thus suggests an equilibration process between El Niño events and their planetary-scale environment (i.e., the warm-pool SST and the associated time-mean climate). Such an equilibration process clearly deserves further study.

This heat pump view of the origin of ENSO appears to shed new light on the question of why El Niño–like phenomena are absent in the Atlantic Ocean. Figure 23

compares the surface heating, SST, depth of the thermocline, and the upper-ocean heat content between the equatorial Pacific and equatorial Atlantic. The equatorial Pacific and the Atlantic have different zonal widths. To isolate the importance of the aforementioned thermodynamical conditions, the relevant quantities are compared on the normalized longitude—the width of the two basins are scaled by their respective zonal width. Figure 23 shows that the Atlantic Ocean has a lower warm-pool SST, weaker surface heating, a less steep thermocline, and a lower equatorial upper-ocean heat content. Thus Fig. 23 suggests that the reason for the absence of El Niño–like phenomena in the Atlantic Ocean is cooler SSTs or the associated lower heat content in the western Atlantic. Again, this explanation differs from but does not contradict the explanation offered by the delayed oscillator hypothesis. According to the delayed oscillator hypothesis, the reason for the absence of El Niño–like phenomena in the tropical Atlantic and Indian Oceans is that a surface warming in the eastern side of the ocean would not have sufficient time to develop before the cooling Kelvin wave emanating from the western boundary kills the warming. How fast the surface warming can grow, however, is unlikely to be independent of the amount of heat accumulated in the equatorial upper ocean.

By delineating the role of warm pool SST in controlling the amplitude of ENSO, the heat pump picture lends support for a possible link between the more energetic El Niños in the last two decades and the anomalously higher warm-pool SST of this period. To the extent the increases in the warm-pool SST can be attributed to global warming, the present results support the view that global warming tends to strengthen the ENSO cycle. We would like to caution, however, that experiments with more sophisticated models need to be done to further test this hypothesis. The present effort with the coupled model is largely limited to providing an example to show that the heat pump hypothesis inferred from observations can be consistent with the first principles that govern the heat and momentum conservation in the equatorial ocean. The ocean model is more sophisticated, but the treatment of atmospheric forcing has not gone significantly beyond earlier theoretical studies (Neelin 1991; Neelin and Jin 1993; Sun and Liu 1996; Sun 1997). Of particular concern is the neglect of seasonal variations in the thermal forcing and the effect of ''weather noise'' in the present investigation. Recent studies using the Zebiak and Cane model have suggested an important role of the seasonal cycle in determining the magnitude of El Niño warming (Clement et al. 1996; Clement et al. 2000). Evidence is also accumulating that weather noise may be an important element in ENSO dynamics (Penland and Sardeshmukh 1995; Eckert and Latif 1997; McPhaden 1999). Nevertheless, the present results complement earlier theoretical studies using an intermediate ocean model that do not explicitly calculate the heat budget of the equatorial subsurface ocean.

The present results suggest that the underestimate of the amplitude of ENSO in the NCAR CSM (Boville and Gent 1998; Meehl and Arblaster 1998) may be linked to the cold bias in the equatorial SST (Kiehl 1998). Recall Fig. 19a in the present article, which shows that the experiment with a higher tropical maximum SST and stronger El Niño events is also warmer across the entire equatorial Pacific. In the same vein, it may not be a coincidence that GCMs that have a cold bias in the equatorial SST also underestimate the magnitude of El Niño events (Davey et al. 2002; Latif et al. 2002).

The present results may also be helpful for better understanding the recent empirical findings of Tudhope et al. (2001). Their inference from coral data of an important role of western Pacific warm pool SST in regulating the amplitude of ENSO may be due to the mechanism delineated here. By revealing a role of El Niño in regulating the stability of the coupled system, the present results also provide a mechanism by which the time-mean state of the equatorial ocean is prevented from being forced substantially away from neutrality.[4] This in turn has implications for the question of why the long-term mean value of the tropical maximum SST appears to have been limited to below a critical value (Crowley and North 1991; Ramanathan and Collins 1991; Pierrehumbert 1995; Sun and Liu 1996). These suggestions need to be further explored with the use of full-blown coupled GCMs. The present study should nicely complement those full-blown GCM studies by serving as a diagnostic framework for better understanding results from those more complex models.

Acknowledgments. The author would like to thank Dr. Randy Dole, Dr. Prashant Sardeshmukh, and Dr. Kevin Trenberth for their encouragements in this research. The author also would like to thank Dr. Peter Gent for providing the code for the ocean model and the initial guidance for how to use the model. The author is grateful to Dr. Richard Seager for his constructive comments in the many email exchanges, and to Dr. Mike Alexander for providing timely feedback for an earlier manuscript. The author also gratefully acknowledges the helpful conversations with Dr. Bette Otto-Bliesner, Dr. Martin Hoerling, Dr. Cecile Penland, Dr. Joe Tribbia, and Dr. Robert Webb. Thanks also go to Mr. Andres Roubicek for his excellent technical assistance. The insightful comments and helpful suggestions from the two anonymous reviewers are also gratefully acknowledged. The author also appreciates Dr. Mojib Latif's editorial effort.

[4] Based on empirical evidence, Penland and Sardeshmukh (1995) argued that the time-mean state of the coupled tropical Pacific ocean–atmosphere system hovers fairly closely to the critical point of stability. They did not investigate, however, what prevents the time-mean state of the coupled tropical ocean–atmosphere from becoming significantly unstable.

This research was partially supported by the National Oceanic and Atmospheric Administration and partially supported by the National Science Foundation climate dynamics program (ATM-9912434).

REFERENCES

Barkstrom, B. R., E. Harrison, G. Smith, R. Green, J. Kibler, R. Cess, and the ERBE Science Team, 1989: Earth Radiation Budget Experiment (ERBE) archival and April 1985 results. *Bull. Amer. Meteor. Soc.*, **70,** 1254–1262.

Battisti, D. S., 1988: Dynamics and thermodynamics of a warming event in a coupled tropical atmosphere–ocean model. *J. Atmos. Sci.*, **45,** 2889–2919.

Boville, B., and P. Gent, 1998: Century integrations with the NCAR CSM version 1. *J. Climate,* **11,** 1115–1130.

Brady, E. C., 1994: Interannual variability of meridional heat transport in a numerical model of the upper equatorial Pacific Ocean. *J. Phys. Oceanogr.*, **24,** 2675–2693.

Cane, M. A., A. C. Clement, A. Kaplan, Y. Kushnir, D. Poznyakov, R. Seager, S. E. Zebiak, and R. Murtugudde, 1997: Twentieth-century sea surface temperature trends. *Science,* **275,** 957–960.

Cess, R. D., and Coauthors, 1990: Intercomparison and interpretation of climate feedback processes in 19 atmospheric general circulation models. *J. Geophys. Res.*, **95,** 16 601–16 615.

Clement, A., R. Seager, M. A. Cane, and S. E. Zebiak, 1996: An ocean dynamical thermostat. *J. Climate,* **9,** 2190–2196.

——, ——, and ——, 2000: Suppression of El Niño during the mid-Holocene by changes in the earth's orbit. *Paleoceanography,* **15,** 731–737.

Crowley, W. P., and G. R. North, 1991: *Paleoclimatology.* Oxford University Press, 339 pp.

Davey, M., and Coauthors, 2002: 1. STOIC: A study of coupled model climatology and variability in tropical ocean regions. *Climate Dyn.*, **18,** 403–420.

Eckert, C., and M. Latif, 1997: Predictability of a stochastically forced hybrid coupled model of El Niño. *J. Climate,* **10,** 1488–1504.

Gent, P. R., 1991: The heat budget of the TOGA-COARE domain in an ocean model. *J. Geophys. Res.*, **96,** 3323–3330.

——, and M. A. Cane, 1989: A reduced gravity, primitive equation model of the upper equatorial ocean. *Comput. Phys.*, **81,** 444–480.

Houghton, J. T., Y. Ding, D. J. Griggs, M. Noguer, P. J. Linden, X. Dai, K. Maskell, and C. A. Johnson, Eds., 2001: *Climate Change 2001: The Scientific Basis.* Cambridge University Press, 881 pp. [Available online at http://www.ipcc.ch/]

Ji, M., A. Leetmaa, and J. Derber, 1995: An ocean analysis system for seasonal to interannual climate studies. *Mon. Wea. Rev.*, **123,** 460–481.

Jin, F.-F., 1997a: An equatorial ocean recharge paradigm for ENSO. Part I: Conceptual model. *J. Atmos. Sci.,* **54,** 811–829.

——, 1997b: An equatorial ocean recharge paradigm for ENSO. Part II: A stripped-down coupled model. *J. Atmos. Sci.*, **54,** 830–847.

Kalnay, E., and Coauthors, 1996: The NCEP/NCAR 40-Year Reanalysis Project. *Bull. Amer. Meteor. Soc.,* **77,** 437–471.

Kiehl, J. T., 1998: Simulation of the tropical Pacific warm-pool with the NCAR climate system model. *J. Climate,* **11,** 1342–1355.

——, J. J. Hack, G. B. Bonan, B. A. Boville, D. L. Williamson, and P. J. Rasch, 1998: The National Center for Atmospheric Research Community Climate Model: CCM3. *J. Climate,* **11,** 1342–1345.

Klinger, B. A., and J. Marotzke, 2000: Meridional heat transport by the subtropical cell. *J. Phys. Oceanogr.*, **30,** 696–705.

Knutson, T. R., S. Manabe, and D. Gu, 1997: Simulated ENSO in a global coupled ocean–atmosphere model: Multidecadal amplitude modulation and CO^2 sensitivity. *J. Climate,* **10,** 131–161.

Latif, M., A. Sterl, E. Majer-Reimer, and W. M. Junge, 1993: Climate variability in a coupled GCM. Part I: The tropical Pacific. *J. Climate,* **6,** 5–21.

——, and Coauthors, 2002: ENSIP: The El Niño simulation intercomparison project. *Climate Dyn.*, **18,** 255–276.

Levitus, S., and T. P. Boyer, 1994: *Temperature.* Vol. 4, *World Ocean Atlas 1994,* NOAA Atlas NESDIS 4, 117 pp.

Liu, Z., S. G. H. Philander, and R. C. Pacanowski, 1994: A GCM study of tropical–subtropical upper ocean mass exchange. *J. Phys. Oceanogr.*, **24,** 2606–2623.

Lu, P., J. P. McCreary Jr., and B. A. Klinger, 1998: Meridional circulation cells and the source waters of the Pacific equatorial undercurrent. *J. Phys. Oceanogr.*, **28,** 62–84.

McCreary, J. P., and P. Lu, 1994: Interaction between the subtropical and the equatorial ocean circulations: The subtropical cell. *J. Phys. Oceanogr.*, **24,** 466–497.

McPhaden, M. J., 1999: Genesis and evolution of the 1997–98 El Niño. *Science,* **283,** 950–954.

Meehl, G. A., and J. M. Arblaster, 1998: The Asian and Australian monsoon and the El Niño–Southern Oscillation in the NCAR climate system model. *J. Climate,* **11,** 1356–1385.

——, P. R. Brantstator, and W. M. Washington, 1993: Tropical Pacific interannual variability and CO_2 climate change. *J. Climate,* **6,** 42–63.

——, P. Gent, J. M. Arblaster, B. Otto-Bliesner, E. Brady, and A. Craig, 2001: Factors that affect amplitude of El Niño in global coupled climate models. *Climate Dyn.*, **17,** 515–526.

Neelin, J. D., 1991: The slow sea surface temperature mode and the fast-wave limit: Analytical theory for tropical interannual oscillations and experiments in a hybrid coupled model. *J. Atmos. Sci.*, **48,** 584–606.

——, and F. F. Jin, 1993: Modes of interannual tropical ocean–atmosphere interaction—A unified view. II: Analytical results in the weak coupling limit. *J. Atmos. Sci.*, **50,** 3054–3522.

——, D. S. Battisti, A. C. Hirst, F. F. Jin, Y. Wakata, T. Yamagata, and S. Zebiak, 1998: ENSO theory. *J. Geophys. Res.*, **103,** 14 261–14 290.

Otto-Bliesner, B. L., and E. C. Brady, 2001: Tropical pacific variability in the NCAR Climate System Model. *J. Climate,* **14,** 3587–3607.

Penland, C., and P. D. Sardeshmukh, 1995: The optimal growth of tropical sea surface temperature anomalies. *J. Climate,* **8,** 1999–2024.

Philander, S. G., 1990: *El Niño, La Niña, and the Southern Oscillation.* Academic Press, 293 pp.

Pierrehumbert, R. T., 1995: Thermostats, radiator fins, and the local runaway greenhouse. *J. Atmos. Sci.*, **52,** 1784–1806.

Ramanathan, V., and W. Collins, 1991: Thermodynamic regulation of ocean warming by cirrus clouds deduced from observations of the 1987 El Niño. *Nature,* **351,** 27–32.

——, B. Subasilar, G. J. Zhang, W. Conant, R. D. Cess, J. T. Kiehl, H. Grassl, and L. Shi, 1995: Warm pool heat budget and shortwave cloud forcing: A missing physics. *Science,* **267,** 499–503.

Rayner, N. A., E. B. Horton, D. E. Parker, C. K. Folland, and R. B. Hackett, 1996: Version 2.2 of the global sea-ice and sea surface temperature data set, 1903–1994. Climate Research Tech. Note 74 (CRTN74), Hadley Centre for Climate Prediction and Research, Met Office, United Kingdom, 35 pp.

Seager, R., and R. Murtugudde, 1997: Ocean dynamics, thermocline adjustment, and regulation of tropical SST. *J. Climate,* **10,** 521–534.

Suarez, M. J., and P. S. Schopf, 1988: A delayed action oscillator for ENSO. *J. Atmos. Sci.*, **45,** 3283–3287.

Sun, D.-Z., 1997: El Niño: A coupled response to radiative heating? *Geophys. Res. Lett.*, **24,** 2031–2034.

——, 2000a: Global climate change and ENSO: A theoretical framework. *El Niño: Historical and Paleoclimatic Aspects of the Southern Oscillation, Multiscale Variability and Global and Regional Impacts,* H. F. Diaz and V. Markgraf, Eds., Cambridge University Press, 443–463.

——, 2000b: The heat sources and sinks of the 1986–87 El Niño. *J. Climate,* **13,** 3533–3550.

——, and Z. Liu, 1996: Dynamic ocean–atmosphere coupling: A thermostat for the Tropics. *Science,* **272,** 1148–1150.

——, and K. E. Trenberth, 1998: Coordinated heat removal from the equatorial Pacific during the 1986–87 El Niño. *Geophys. Res. Lett.,* **25,** 2659–2662.

Tett, S., 1995: Simulation of El Niño–Southern Oscillation-like variability in a global AOGCM and its response to CO_2 increase. *J. Climate,* **8,** 1473–1502.

Timmermann, A., J. Oberhuber, A. Bacher, M. Esch, M. Latif, and E. Roeckner, 1999: Increased El Niño frequency in a climate model forced by future greenhouse warming. *Nature,* **398,** 694–697.

Trenberth, K. E., 1997: Using atmospheric budgets as a constraint on surface fluxes. *J. Climate,* **10,** 2796–2809.

——, J. M. Caron, and D. P. Stepaniak, 2001: The atmospheric energy budget and implications for surface fluxes and ocean heat transports. *Climate Dyn.,* **17,** 259–276.

Tudhope, A. W., and Coauthors, 2001: Variability in the El Niño–Southern Oscillation through a glacial–interglacial cycle. *Science,* **291,** 1511–1517.

Weare, B. C., P. T. Strub, and M. D. Samuel, 1981: Annual mean surface heat fluxes in the tropical Pacific Ocean. *J. Phys. Oceanogr.,* **11,** 705–717.

Wyrtki, K., 1985: Water displacements in the Pacific and the genesis of El Niño cycles. *J. Geophys. Res.,* **90,** 7129–7132.

Xu, K.-M., and K. Emanuel, 1989: Is the tropical atmosphere conditionally unstable? *Mon. Wea. Rev.,* **117,** 1471–1479.

Zebiak, S. E., and M. A. Cane, 1987: A model El Niño–Southern Oscillation. *Mon. Wea. Rev.,* **115,** 2262–2278.

——, and ——, 1991: Natural climate variability in a coupled model. *Greenhouse-Gas-Induced Climatic Change: A Critical Appraisal of Simulations and Observations,* M.E. Schlesinger, Ed., Elsevier, 457–469.

Zhang, Y., J. M. Wallace, and D. S. Battisti, 1997: ENSO-like interdecadal variability. *J. Climate,* **10,** 1004–1020.